Agriculture, Ecosystems and Environment 411 (2026) 110623

Contents lists available at ScienceDirect

Agriculture, Ecosystems and Environment

journal homepage: www.elsevier.com/locate/agee

High-resolution N_2O and CH_4 emissions during cabbage and fallow seasons in a paddy soil in Vietnam

Lara Melissa Fritzsche [a,b,1], Hans Frederik Engvej Hansen [a,1], David Kraus [c], Marija Popovic [a], Rosa Elvira Hvidsten Gregersen [a], Klaus Steenberg Larsen [d], Vu Duong Quynh [e], Mai Van Trinh [e], Nguyen Thi Oanh [e], Bo Elberling [a,*]

[a] Global Wetland Center, Dept. of Geosciences and Natural Resource Management, University of Copenhagen, Øster Voldgade 10, København K 1350, Denmark
[b] Dept. of Plant and Environmental Sciences, University of Copenhagen, Frederiksberg C 1871, Denmark
[c] Institute of Meteorology and Climate Research, Atmospheric Environmental Research (IMK-IFU) KIT - The Research University in the Helmholtz Association, Kreuzeckbahnstr. 19, Garmisch-Partenkirchen, 82467, Germany
[d] Dept. of Geosciences and Natural Resource Management, University of Copenhagen, Rolighedsvej 23, Frederiksberg C 1958, Denmark
[e] Institute for Agricultural Environment, Vietnam Academy of Agricultural Sciences, Sadoi Street, Phudo, South Tu Liem, Hanoi, Viet Nam

ARTICLE INFO

Dataset link: emissions and soil measurements

Keywords:
Paddy soils
Rice–vegetable rotation system
N_2O emissions
Hot moment
LandscapeDNDC

ABSTRACT

Rice paddy soils are a significant source of methane (CH_4). Nitrous oxide (N_2O) is another potent greenhouse gas (GHG) but its significance to GHG balance in rice paddies remains uncertain. Here, we present high-resolution measurements of CH_4 and N_2O using automated chambers, combined with subsurface O_2 concentrations, over a fallow period and a cabbage-growing season in a subtropical rice-vegetable rotation system. The combination of automated chambers, subsurface oxygen profiling, and LandscapeDNDC modelling calibrated to measured O_2 dynamics provides unprecedented mechanistic insight into N_2O hot moments in rice–vegetable rotations. Episodic "hot moments" dominated N_2O emissions, with 72% of total seasonal flux occurring within 27% of the cabbage season. Mean and peak N_2O fluxes during cabbage cultivation reached 104 μg N_2O-N m^{-2} h^{-1} and 682 μg N_2O-N m^{-2} h^{-1}, respectively. High-emission events were linked to fertilisation, changes in water-filled pore space and subsurface oxygen availability, with N_2O fluxes initially dominated by denitrification under saturated conditions and later by nitrification as nitrate and oxygen increased and ammonium decreased. This conclusion was supported by LandscapeDNDC. The emission factor for nitrogen applied was 0.52%, and nitrogen use efficiency was 38%. Total N_2O emissions during cabbage cultivation were sevenfold higher than fallow, whereas CH_4 fluxes remained unchanged. The global warming potential (GWP) in cabbage was driven by N_2O rather than CH_4. These findings highlight the importance of capturing N_2O emission events in paddy-to-vegetable transition systems and the value of process-based modelling to identify dominant biogeochemical pathways.

1. Introduction

Rice is an essential food crop and the primary food source for more than 3.5 billion people, providing more than 20% of their daily calorie intake (IRRI, 2024; Sumithra et al., 2014). Between 1990 and 2019, the global harvested area of rice has increased by 11%, while production of rice grown in paddy soils rose by 46% (Intergovernmental Panel On Climate Change Ipcc, 2021).

Rice production, particularly from flooded rice paddies, is a major agricultural source of CH_4 due to anaerobic soil conditions but contributes also to N_2O emissions through nitrification and denitrification (Intergovernmental Panel On Climate Change Ipcc, 2021). Rice production is the second largest anthropogenic source of CH_4 globally, after enteric fermentation from livestock (Intergovernmental Panel On Climate Change Ipcc, 2021; Tirol-Padre et al., 2017). While CH_4 emissions from flooded rice paddies have long received much attention due to their high emissions under anaerobic conditions, recent research highlights the importance of N_2O emissions as well. This shift is due to

* Corresponding author.
E-mail addresses: fzg118@alumni.ku.dk (L.M. Fritzsche), hfeh@ign.ku.dk (H.F.E. Hansen), david.kraus@kit.edu (D. Kraus), ksl@ign.ku.dk (K.S. Larsen), be@ign.ku.dk (B. Elberling).
[1] Shared first-authorship

https://doi.org/10.1016/j.agee.2026.110623
Received 13 February 2026; Received in revised form 10 May 2026; Accepted 26 June 2026
Available online 9 July 2026

N_2O's high GWP and complex response to management practices (Intergovernmental Panel On Climate Change Ipcc, 2021). About 43% of the total N_2O emissions are of anthropogenic origin, of which agriculture is the largest source, accounting for 52% (Tian et al., 2020). Global emissions are increasing with the rising demand for agricultural production, making it crucial to investigate their impact and provide guidelines for future land use practices to minimize their environmental and climatic impact. This is especially relevant since current mitigation strategies targeting CH_4, such as drainage, can increase N_2O emissions (Sander et al., 2016).

A common and effective cultivation method is the rice variety *Oryza Sativa* grown in paddy soils. Paddy soils are characterized by a hardpan layer with low permeability at 10–25 cm depth (Hamada et al., 2021). Rice paddies are levelled and surrounded by earthen or plastic bunds, with water levels controlled through channels around the fields. Current practice is labour intensive, with unique tasks such as water management, transplanting seedlings, fertilizer management, pest and disease management, and keeping the bunds intact.

In many regions, rice is cultivated multiple cycles per year, with some areas reaching up to three cycles annually. As this intensive cultivation can put pressure on soil health and water resources, crop rotation is a common practice in paddy soils. Crop rotation provides several benefits, including pest and disease control, improved nutrient availability, and prevention of soil degradation (Zhang et al., 2022). Typical rotation crops include vegetables, legumes, and oilseeds, while fallow periods are often incorporated as well (Kumar et al., 2020; Linh et al., 2017). As these crops and fallow periods contribute to the annual GHG budget, they should be studied and included in annual GHG budget to understand variations in GHGs across different farming systems. Notably, fallow periods can contribute substantially to emissions, with studies reporting elevated CH_4 and N_2O fluxes during fallow periods (Gaihre et al., 2018).

CH_4 is produced via methanogenesis under anaerobic conditions by methanogenic archaea. The main pathways include acetoclastic methanogenesis and hydrogenotrophic methanogenesis with the former accounting for the majority of CH_4 production in rice paddies (Conrad, 2007). In paddy soils, clayey water-logged soils, combined with the aerenchyma pathway, provide optimal conditions for CH_4 production and emissions. However, optimized water management can significantly reduce emissions. The management practice of alternating wetting and drying (AWD) is becoming more widespread. The principle is to alternate from a flooded field to periods of natural drainage and evaporation, that create periods of low water table (Bouman and Tuong, 2001). During dry periods, the soil becomes unsaturated and partly oxidized and consequently CH_4 production is prevented in the unsaturated soil layers. Additionally, a zone of CH_4 oxidation may form below the unsaturated zone. If applied correctly, it has been found to reduce emissions by 20–30% without compromising yields and has the further advantage of saving water (Intergovernmental Panel On Climate Change Ipcc, 2021). However, it requires additional labour and expertise for proper implementation compared to traditional farming practices.

Importantly, Kritee et al. (2018) demonstrated that N_2O emissions from intermittently flooded rice fields could be 30–45 times higher than reported under continuous flooding and therefore at least partly may counterbalance the reductions in CH_4 emissions. N_2O emissions from paddy rice have been reported in a broad range of 0.13–654 μg N_2O-N m^{-2} hr^{-1} (Akiyama et al., 2005; Kritee et al., 2018) and known to be controlled by both soil moisture, nitrogen (N), and carbon (C) availability (Ju et al., 2024; Liao et al., 2021; Weier et al., 1993). Emission factors (EF) range from 0.3% (continuous flooding) to 0.5% (multiple drainage) according to Intergovernmental Panel On Climate Change Ipcc, (2019).

Urea fertilizers are extensively used in rice paddies, which breaks down in the soil to release ammonium ions (NH_4^+) or undergoes nitrification to produce nitrate (NO_3^-), which both can be taken up by plants (Hachiya and Sakakibara, 2016). However, plant N uptake efficiency (NUE) is typically only 40–50% or less (Ladha et al., 2005; Raun and Johnson, 1999), leaving excess N that can be lost to the environment in the form of gasses (ammonia (NH_3), dinitrogen (N_2), and N_2O) or it is leached as NO_3^- to streams, rivers, and lakes where it often leads to severe pollution (Wang et al., 2019).

Fertilizer type, amount, timing, and application method all influence N_2O emissions where nitrification and denitrification are involved. Under the process of nitrification, low oxygen or high NH_4^+ concentration can lead to incomplete oxidation of NH_2OH and produce N_2O (Bernhard, 2010). Under denitrification N_2O exists as an intermediate. N_2O is emitted when conditions of low pH or limited C inhibit the final reduction to N_2 (Pandey et al., 2014; Pfeifer-Meister et al., 2018). These conditions are strongly influenced by water management in rice paddies. When rice paddies are kept continuously flooded, nitrification is inhibited, and no NO_3^- is available for denitrification process. Furthermore, anaerobic conditions favour the denitrification process to go to completion producing N_2 instead of N_2O (Bollmann and Conrad, 1998). However, when drainage is periodically applied, e.g. as part of AWD management, redox potentials fluctuate, which creates optimal conditions for both nitrification and denitrification, leading to high N_2O emissions (Sriphirom et al., 2019).

Short periods account for a high percentage of the total N_2O emissions and are referred to as hot moments (Krichels and Yang, 2019; McClain et al., 2003). Combined with the fact that much is unknown about N_2O emission patterns, these events have been challenging to capture, and high emissions may have been missed. The most dominant method to measure N_2O emissions in the field to date is using manual static chambers. This method is simple and effective for doing snapshot measurements, but it is labour intensive and has limited temporal resolution (Barton et al., 2015; Savage et al., 2014). Thus, automatic chambers that measure with high temporal resolution are gaining more interest. Consequently, N_2O assessments may be biased due to both lack of measurements outside the main rice season and lack of high-resolution data, i.e. especially hot moments are not fully accounted for when measurements are performed with manual chambers.

Few studies have investigated both N_2O and CH_4 emissions from rice paddies (Zou et al., 2007; Kim et al., 2021; Ju et al., 2024) using manual chambers. A typical measurement cycle for manual chambers is once a week, while automatic chambers can measure multiple times per day. While a few studies have managed to capture hot moments using manual chambers, a high temporal resolution is important to quantify the importance of hot moments (Liu et al., 2023). Finally, almost no data exists for the periods where rice paddies are cropped with vegetables or left as fallow – despite that these periods in the Red River Delta account for around 25% of the time. Optimal climate mitigation strategies for paddy soils can only be developed if GHG fluxes from all the different crops used in paddy cropping systems are investigated.

Objectives for this study aims were to identify and quantify underlying processes controlling N_2O emissions from a season of cabbage and fallow, including quantifying the importance of "hot moments" from a representative site of the Red River Delta (RRD) in North Vietnam. To fulfil the objectives, we have combined high-resolution measurements of CH_4 and N_2O fluxes using automated chambers combined with subsurface O_2 concentrations and finally applied the LandscapeDNDC biogeochemical model to improve the understanding of underlying processes for observed N_2O emissions.

It is hypothesised that fertilization outside the main rice seasons plays an important role for both the annual N budget and N_2O emissions in paddy soils of the Red River Delta, and secondly that N_2O emissions are biased and poorly constrained despite the importance for recommendation for land use practices in addition to CH_4.

2. Methods

2.1. Study site

Vietnam is the fifth largest producer of rice worldwide, with an annual production of approximately 43.5 million tons (FAO, 2024). Around 21% of the country's area is used for rice production (FAO, 2024). RRD is known for its extensive rice cultivation and is the second most important agricultural area in Vietnam, after the Mekong Delta in the south of Vietnam. RRD accounts for 18% of the national rice production and about 3 months a year paddy soils in RRD are used for growing vegetables or left for fallow (Huy, 2025; Thanh, 2025). Due to its fast-growing population, expanding industrial sector, and strong economic progress, this region is a representative case of advanced and modernized rice farming (Luu et al., 2010). The experimental field site is located in Bac Tien Hung commune, Hưng Yên province, Vietnam, with the coordinates being 20°34'35.1"N, 106°19'32.4"E (Fig. 1; Figs. S1-2). About 78% of area is allocated agricultural production of which 80% is rice (299 ha) (Huy et al., 2024; Trang et al., 2019). Spring rice yields reach 7.3 tons ha^{-1} and summer rice yields reach 6.3 tons ha^{-1} (Trang et al., 2019). Hưng Yên province is one of the major rice producers in Vietnam (Linh, 2024).

The experimental site covers an area of 1800 m^2. The field site has been used for cultivation of mainly rice the last hundred years (Thanh, 2025). According to the soil map of the National Institute for Soils and Fertilizers (2002), the site is of alluvial soil, typically known as fertile, mineral-rich soil formed by river-borne sediments, with a loamy texture and good drainage (FAO, 2024; Fig. 1).

The experimental site is part of the Red River Delta (RRD) and its tributaries. It is one of the most densely populated regions in Vietnam and is home to close to 24% of the whole country's population, including the capital of Hanoi (General Statistics Office of Vietnam, 2025). The RRD is located within a tropical monsoon climate according to Köppen-Geiger climate classification (Beck et al., 2023). The climate is dominated by three seasons: The cool and dry season (October-January), the cool and humid season (February-April), and the hot and wet season (May–September) according to Huong et al. (2013). The rain season typically lasts from May to October and dry season from November to April.

More than 50% of RRD is characterised by alluvial soils (Fig. 1), a medium texture silty soil with a light brown colour and a neutral pH and considered suitable for rice production (Huong et al., 2013). Agriculture in the Red River Delta is dominated by rice cultivation, but the region also produces 26% of Vietnam's vegetables (Huong et al., 2013; Morton, 2020). Annual crops occupy 90% (6700 km^2) of the land, supported by RRD's dense networks of rivers, canals, ditches, sluice gates, and compartmented fields (Morton, 2020). Rice is cultivated twice per year, and during the colder months, either alternative crops, such as vegetables, are grown, or the fields are left fallow.

2.2. Weather and climate data

An on-site meteorological station (RIKA900–10 ultrasonic, Rika Sensors, Changsha, China) monitoring precipitation, air temperature, humidity, and windspeed was placed approximately 10 m away from the chambers. Additional meteorological data was made available from a permanent meteorological station located approximately 17 km away from the field site in Vũ Ninh (20°25'34.3"N, 106°22'29.3"E).

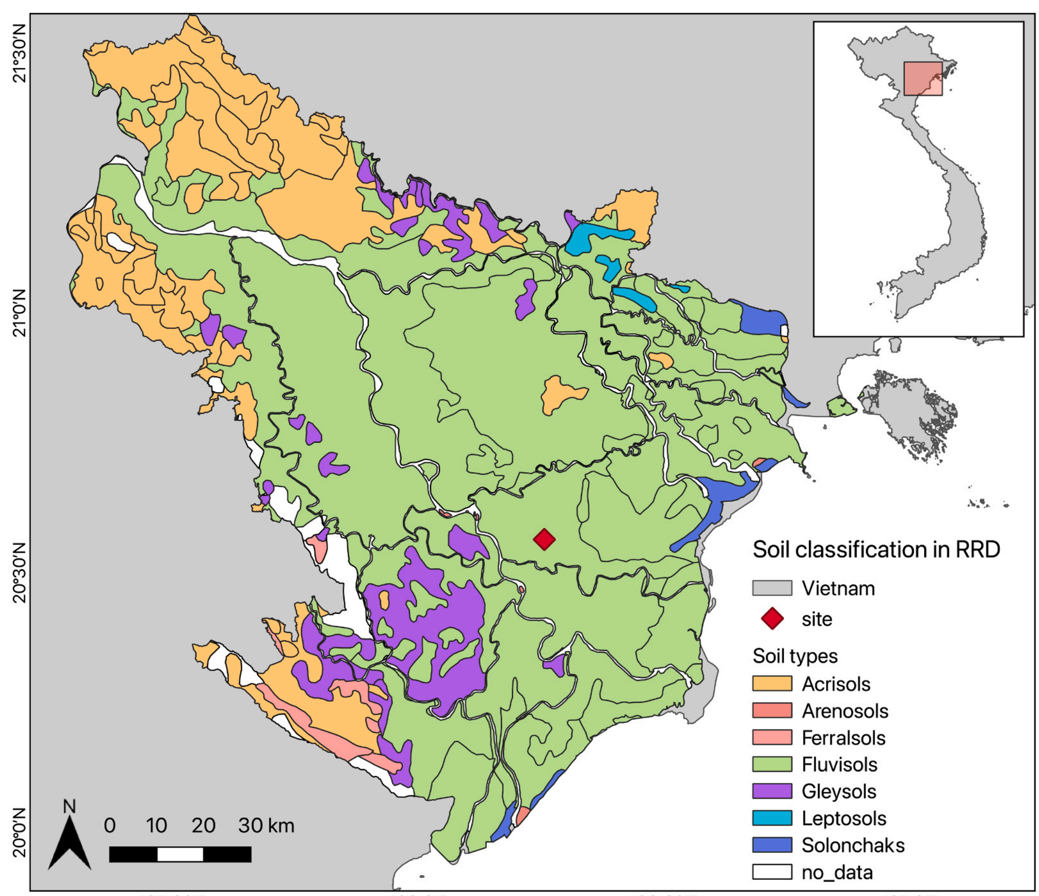

Fig. 1. A map with soil types showing the location of the experimental site (marked with a red diamond) in Bac Tien Hung commune, Hưng Yên province, Vietnam. Map of the soil classifications is based on data from Soils and Fertilizers Research Institute and subsequently processed in QGIS.

Due to overheating, the on-site meteorological station did not record data between 15 November 2024 and 21 November 2024, precipitation was not recorded between 17 November 2024 and 23 November 2024 and soil temperature was not recorded between 15 November 2024 and 23 November 2024. To fill the data gaps, data from the on-site station were plotted against the data from the permanent meteorological station and linear regressions of these plots were used for gap filling (Fig. S3, S4, S5, and Table S1). Soil moisture was not recorded between 16 November 2024 and 23 November 2024 but could not be gap filled and periods of missing data are therefore indicated by dashed lines in graphs.

2.3. Soil characteristics

Prior to the beginning of the experiment, soil samples were taken (28 October 2024) to a depth of 1 m, with 100 cm^2 volumetric rings (layered sampling at 0–6.1 cm, 6.1–12.2 cm etc. with 3 replicates per layer, Fig. 2S). Based on the total weight of volume-specific samples and subsamples before and after drying for 48 h, the water content and bulk density were calculated. Soil pH was measured directly in soil water extractions, using fresh moist soil to water ratio of 1:5. Deionized water was added, and the mix was shaken for 1 h at room temperature. Afterwards it was centrifuged and finally filtered through a 5 µm membrane filter before measurement (pHenomenal pH 1100 LTM, VWR, Darmstadt, Germany). After drying the subsamples were finely ground and analysed for total C and as total N using a Eurovector elemental analyser (Redavalle, Italy) coupled to Isoprime (Isoprime Ltd., Cheadle Hulme, UK) isotope ratio mass spectrometer (IRMS). Depth-integrated soil pools were calculated based on soil bulk density and content of soil C. Grain size distributions were measured using a Bandelin Sonopuls HD2200 Sonifier and Malvern Mastersizer 2000.

2.4. The experimental set-up

The experimental set-up consists of 6 automatic ECOFlux chambers, ver. 3.0, DMR (Prenart Equipment ApS, see www.prenart.dk, Copenhagen, Denmark supported by Gaia2Tech Aps, Frederikssund, Denmark, Fig. 2a, S1, and S2). See Tariq et al. (2022) for further details. Chambers were located approximately 2–3 m away from each other in two blocks 5 five m apart. The chamber area was 3058 cm^2 and had an average height of 93 cm giving an internal volume of 291 L. When measuring N_2O and CH_4 fluxes, one chamber at the time was closed by a lid and connected in a closed loop to an ultra-portable N_2O-CH_4 analyser (N2OM1–919, Los Gatos Research, Ca USA), measuring the concentration in the chamber headspace at 1 Hz. The total measurement (closure) time was 5 min, and in the measurement cycle the tubes were purged for a total of 150 s before and after measurements. The minimum detectable flux was estimated using goFlux and was approximately 0.1 µg N_2O/CH_4 m^{-2} h^{-1} (Christiansen et al., 2015; Rheault et al., 2024). A fan inside the chamber was used to circulate headspace air to ensure mixing and prevent buildup of any concentration gradients. The chambers were also fitted with a vent to prevent pressure build up. A total of 20 measurements (10 light and 10 dark) were conducted per chamber per day and were done shifting between dark and light mode. The same chamber was measured every 2.5 h. Inside each chamber there were placed photosynthetically active radiation (PAR) sensor (Apogee SQ−205-SS), sensors that measure air temperature and humidity inside the chamber (Vaisala HMP 110), as well as soil probes that measure moisture and temperature (Treubner SMT 100) at a depth interval of 1.5–3.5 cm (three replicates per treatment).

Additional in situ sensors were installed to monitor soil environmental conditions. Soil temperature and volumetric water content were measured at depths of 5, 10, 20, 30, and 40 cm using capacitive dielectric sensors (Truebner SMT100). Soil oxygen concentrations were recorded at the same depths using optical oxygen sensors (PreSens Precision Sensing OxyBase). Water table depth (to approximately 32 cm) was monitored using a submersible hydrostatic pressure transducer. Sensors were installed adjacent to one cabbage chamber and one fallow chamber, providing one replicate per treatment.

All soil oxygen sensors were calibrated to a 0% O_2 baseline to correct for potential sensor offsets. Calibration was performed by submerging the sensors in deoxygenated water, thereby establishing anoxic reference conditions. We recorded all variables at 1 Hz, and to reduce noise we applied a moving average (30 s window). Each measurement was given a time stamp to enable aligning with fluxes.

This project compared a season of Green Cabbage (*Brassica oleracea L.*) with a fallow season, each established after rice cultivation. These will be referred to as treatments cabbage and fallow throughout this paper. Three chambers had 2 cabbages each planted inside on 01 November 2024 (representing the average density at nearby fields of approximately 20 cm in between cabbages), while the other three chambers were left as fallow (three replications per treatment (cabbage and fallow), Fig. 2b). The three chambers containing cabbage received urea fertilizer dissolved in water with a total amount of approximately 900 kg N ha^{-1} split into three equal applications on 05 November 2024, 25 December 2024, and 10 January 2025 (Đạm Hà Bắc, produced by Vinachem, Vietnam) and one application of 100 kg P ha^{-1} Single Super Phosphate fertilizer on 12 November 2024 (Supe Lân Lâm Thao, produced by Lâm Thao Fertilizers and Chemicals JSC, Vietnam) all added with a watering can (Fig. 2b). They were irrigated as needed manually. The fallow chambers received no treatment. Prior to planting, the soil in

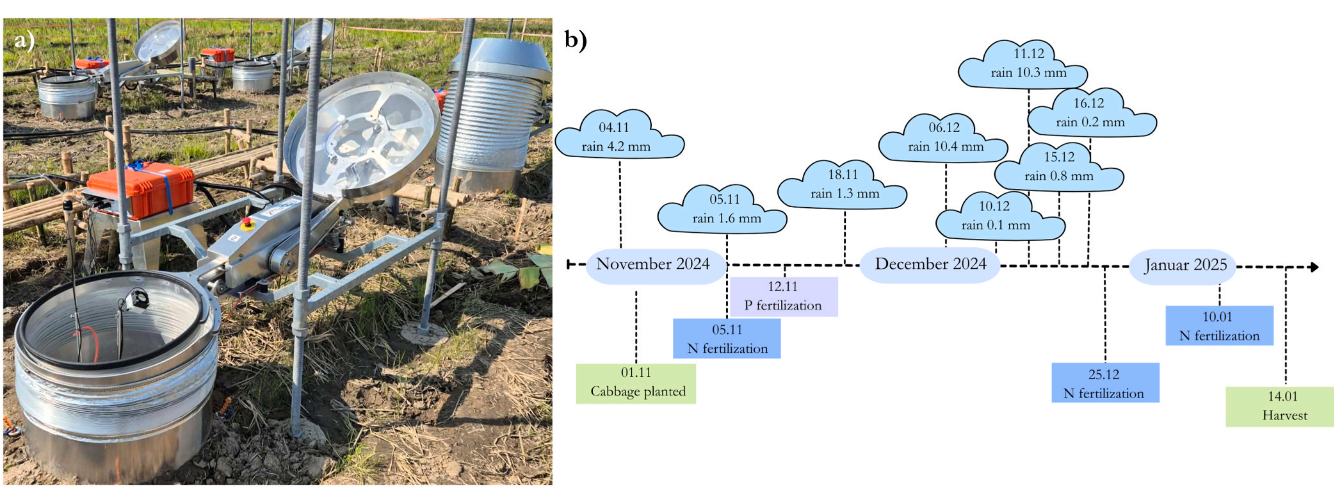

Fig. 2. a) Photo of the automated chambers at the experimental site. b) Timeline of the experimental period including planting of cabbage, harvest of cabbage, fertilization, and rain events.

all chambers was ploughed manually. Weeds were removed by hand throughout the season in all chambers. The remaining field was left fallow, apart from 3 plots next to the chambers containing cabbage with 2 cabbages per plot for soil sampling. Those underwent the same treatments as chamber containing cabbage. The cabbage was harvested on 14 January 2025.

2.5. Weekly manual measurements and sampling

Weekly soil samples were taken next to each chamber at depths 0–2 cm and 13–15 cm in the before mentioned plots with and without cabbage. Fresh soil samples were extracted using 20–25 mL HPLC water in 50 mL extraction tubes with screw caps. They were hand shaken for approximately 1 min. The samples were left for precipitation overnight and were filtered through filter paper (3–13 µm, VWR International). After measuring pH, samples were stored in 15 mL blue tubes in the freezer until analysed at UCPH Department of Geosciences and Natural Resource Management in Copenhagen on 25 April 2025. The extracted samples were analysed for NO_3^- and NH_4^+ using flow-injection analysis (Tecator 5000 FIAStar, Höganäs, Sweden).

2.6. LandscapeDNDC modelling

We conducted a modelling study to investigate how the current representations of nitrification and denitrification in a state-of-the-art process-based model can explain the observed N_2O emissions, and how explicitly constraining soil O_2, an essential but rarely used field constraint for these processes, affects this interpretation.

We used the process based biogeochemical model LandscapeDNDC (version 1.37.0), which has previously been successfully applied to simulate CH_4 and N_2O emissions from paddy rice systems (Kraus et al., 2015; 2016; Nguyen et al., 2026). LandscapeDNDC simulates carbon and nitrogen cycling, including greenhouse gas emissions, in agricultural and natural ecosystems (Haas et al., 2013; Molina-Herrera et al., 2016). The model was initialised with site specific physical and chemical soil properties such as soil texture, clay content, bulk density, pH and soil organic carbon (see Table S12). Further driving data included daily air temperature, precipitation and radiation, as well as agricultural management (fertilisation, tillage, planting, harvesting and water management).

Because only a single season of data was available, we restrained the analysis to an explanatory model behaviour study using a three step, sequential constraining approach. First, depth resolved soil water content measurements at 5, 10, 20, 30, and 40 cm were used to constrain soil hydraulic properties (van Genuchten α and n) and thereby to define realistic hydrological boundary conditions, recognising that soil water content strongly controls gas diffusivity and thus O_2 dynamics. Second, we constrained soil gas diffusivity using measured soil O_2 at 5 cm depth, with the aim of establishing the most plausible topsoil O_2 regime for nitrification and denitrification. Third, we analyseed how LandscapeDNDC, with its current process formulation, must adjust nitrification and denitrification parameters to best reproduce the observed N_2O flux dynamics. This final step intended to derive a process consistent explanation of the N_2O peak and subsequent decline, conditional on the hydrological and O_2 constraints established in the first two steps.

Process models such as LandscapeDNDC contain numerous equations and parameters to represent the underlying system complexity. This can lead to equifinality (Houska et al., 2017), whereby different parameter sets produce similar results, particularly when calibration data are limited. To focus on the role of O_2 in (de)nitrification, we deliberately restricted the number of parameters and processes under investigation:

The effective soil gas diffusivity (D_{eff}) was computed in the MeTrx model using the equation:

$$D_{eff} = \theta_g^{\Omega_{MDEEA}} \quad (3)$$

where θ_g is the soil gas content and Ω_{MDEEA} is a model parameter (technical name: METRX_D_EFF_EXP_AIR). This parameter was constrained against observed O_2 concentrations at 5 cm depth, particularly focusing on the rate of topsoil O_2 increase following field drainage. Key parameters controlling nitrification and denitrification were then adjusted to reproduce the measured N_2O fluxes. This included the soil anaerobic volume fraction (V_{an}), calculated as:

$$V_{an} = e^{-\left(\Omega_{MFS2} \quad p_{O_2}^{\Omega_{MFS1}}\right)} \quad (4)$$

where p_{O2} is the O_2 partial pressure, Ω_{MFS1} and Ω_{MFS2}(METRX_F_SANVF1, METRX_F_SANVF2) are model parameters. The soil anaerobic volume fraction is a key state variable that regulates the share of aerobic processes (e.g., nitrification) and anaerobic processes (e.g., denitrification) and is thus central to our analysis of O_2 effects on N_2O production. Denitrification-specific parameters considered were Ω_{MMEAR} (METRX_MIC_EFF_ANAEROBIC_RESPIRATION), which controls the relation between assimilative and dissimilative carbon use of denitrifying microbes, Ω_{MFDN2}(METRX_F_DENIT_N2_2), which regulates complete denitrification to N_2, and Ω_{MFDMW1} (METRX_F_DENIT_M_WEIBULL_1), which modulates denitrifier activity as a function of soil water. Together, these parameters determine the overall strength of denitrification, its dependence on soil moisture, and the partitioning between N_2O and N_2 production. For nitrification-related N_2O emissions, two key parameters were considered: Ω_{MFNFM} (METRX_F_NIT_FRAC_MIC), which controls the pool size of nitrifying microbes, and Ω_{MKNNN} (METRX_KF_NIT_NO_N2O), which defines the fraction of NH_4^+ undergoing nitrification that is converted to NO and N_2O via chemical decomposition of metabolites and nitrifier-denitrification.

2.7. Harvesting

All 12 cabbages were harvested on 14 January 2025. Dry weight was determined for all cabbages and split into roots, cabbage head, and leaves including the stem. Representative subsamples, collected using the pyramid method of approximately 50 g, were kept in the oven for around 24 h until the weight stabilized. Samples were subsequently kept frozen until analysis. Subsamples from all three fractions were grounded with an agate mortar vibration mill. The roots required additional grinding in a Retsch MM400 mixing mill using stainless steel mortars. The C and N analysis was performed using a Flash 2000 Organic Elemental Analyzer (Thermo Scientific).

2.8. Data analysis and statistics

Data analysis was performed with the software R version 4.4.1 (2024–06–14 ucrt). The raw data from the Ecoflux chambers reports N_2O and CH_4 concentrations in ppb per second. Using the R package goflux (Rheault et al., 2024) both a linear slope and a non-linear slope were estimated (Hutchinson and Mosier, 1981). The deadband was set to 90 s to account for system noise associated with chamber closure, gas transport to the analyser, and potential internal lag within the analyser. This duration was determined based on visual inspection of the measurement time series. Fluxes reported here were calculated using the linear regression method, consistent with most reported fluxes for paddy soils and because non-linear exponential models such as the Hutchinson-Mosier model (HM) may lead to overestimation of fluxes if based on short measurement times (Johannesson et al., 2024). Using the slope and applying the following term fluxes per measurement per chamber were calculated as:

$$flux = \frac{V \times P}{A \times R \times T} \times S \quad (1)$$

where V is the volume of the chamber in cm^3, P is the pressure in kPa, A is the area in cm^2, R is the relative gas constant in $m^3 \times$ kPa /mol $\times$ k, T

is the temperature in Kelvin, and S is the slope of the headspace concentration (ppb s^{-1} or ppm s^{-1}).

Following flux calculation, all flux time series were subjected to visual quality control. Observations exhibiting clear technical or mechanical artefacts attributable to instrumentation malfunction were excluded from further analysis. By default, all remaining measurements were retained. However, fluxes of exceptionally high magnitude were additionally scrutinised on a case-by-case basis and were only excluded if there was clear evidence of poor data quality or measurement failure. Fluxes below the detection limit were included in the analysis. During the growing season, 10,656 measurements were scheduled for each gas. Of these, 1.8% of completed measurements were excluded during post-processing, while 11.1% (CH_4) and 11.6% (N_2O) were not completed due to technical issues. Consequently, 86.8% of scheduled measurements were included in the analysis (Table S14).

For reporting total emission, daily means were calculated and summed across the period 01 November 2024–14 January 2025. For calculating CO_2 equivalents the latest IPCC values of 273 and 27 are used for N_2O and CH_4, respectively (Intergovernmental Panel On Climate Change Ipcc, 2021).

The emission factor was calculated as

$$EF = \frac{N_2O - N\ emitted\ cabbage - N_2O - N\ emitted\ fallow}{N\ applied} \times 100 \qquad (2)$$

Data from sensors was averaged each 5 s and the daily mean is reported.

All statistical tests were performed in R. Welch's two-sample *t*-tests were used to determine differences of means (total weight, water content, C, and N content) between plants outside and inside the chambers. N_2O and CH_4 fluxes were analysed using two complementary approaches. First, fluxes were averaged over time for each chamber and compared between treatments using Welch's two-sample *t*-tests. Second, repeated measurements over time were analysed using a linear mixed-effects model (lmer function from the lme4 package in R implemented by Bates et al. 2015), with treatment, time, and their interaction as fixed effects, and chamber as a random effect with both random intercepts and slopes for time. Model assumptions were controlled by performing model diagnostics including a residuals vs fitted plot and QQ-plots for residuals as well as random effects. No data transformations were applied.

A linear mixed model was also fit to examine differences in NO_3^- and NH_4^+ concentration across treatment, time and depth, including controlling above mentioned model assumptions. Tests were significant if $p < 0.05$. To identify hot moments, the 1.5 × interquartile range (IQR) was calculated with the upper threshold defining a hot moment (as in Stuchiner et al. 2025). A two-dimensional interpolation was performed using the mba.surf function from the MBA (Multilevel B-spline Approximation) package in R (implemented by Øyvind after method of Lee et al., 1997) using the average O_2 concentrations. A 100 × 100 grid was applied, which resulted in estimated oxygen concentration for each 0.74 day and each 0.4 cm. Plant N uptake was calculated by relating average N content to total dry biomass per area and comparing the results to total N input, to estimate uptake efficiency.

3. Results

3.1. Climate and soil characteristics

Daily mean temperatures in the experimental period ranged from 13.7 to 27.9°C (November-January) with a mean temperature of 20.9°C (Fig. S6a). The total rainfall in November and December was 18.9 mm, while there was no rain in January until harvest on 14 January 2025. Compared to climate data from the years 2010–2024 (Fig. 3 and S7) rainfall during this experimental season (November-December) was 65.5 mm lower. The mean temperature was 1.5°C warmer in this experimental period (including January). Over the period between 2010 and 2024, positive significant trends in temperature were found for June and July, while a positive trend in precipitation was found for September and a negative trend for December. Precipitation and air temperature during the experimental period did not differ significantly from the 2010–2024 reference period (all months ≤ 0.64, df = 13, p ≥ 0.53; Fig. S7).

The soil temperature followed the air temperature pattern and decreased over the cabbage season (Fig. S6c). Temperature increased with soil depth. Soil moisture peaked in the beginning of November with a WFPS of close to 90% at a depth of 20 cm followed a rain event (Fig. S6a). Throughout the season, WFPS decreased and stabilized in December and January for all depths, with the deeper soil levels generally having higher WFPS. The highest water levels were recorded in the same period, with a peak of around 10 cm below soil surface (Fig. S6b). From December and on levels were dropping with values of around 32 cm or lower.

Results of soil analyses (summarized in Table 1 and shown as soil profiles in Fig. S8) indicate that soil pH increased with depth from 5 and below the ploughing layer to about 7.5 while bulk density increased in the upper 50 cm and decreased below. Total C was highest in the upper 30 cm and decreased to close to zero below 30 cm. The C:N revealed a similar marked shift in 30 cm. The grain size distribution was dominated

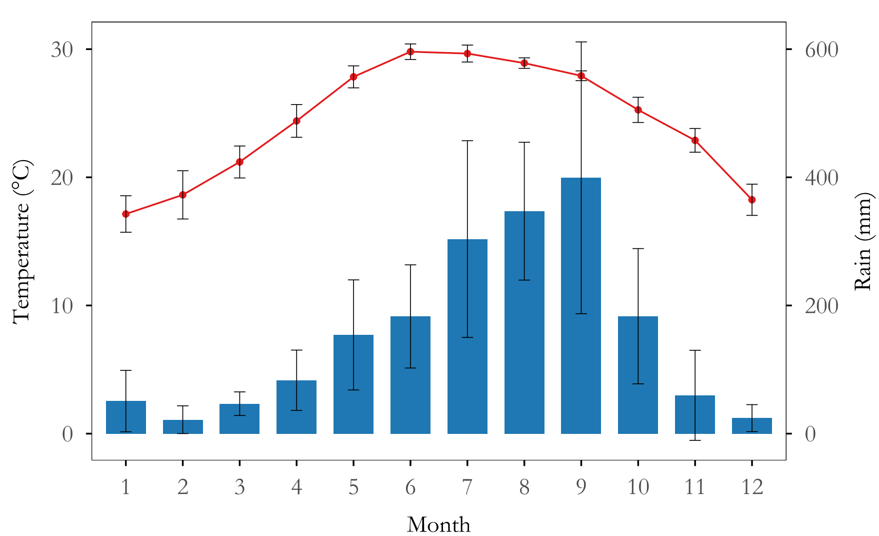

Fig. 3. Mean monthly total rainfall (mm) (blue bars) and temperature (°C) (red line) with standard deviations for 2010–2024 (Vũ Ninh meteorological station).

Table 1
Physical and chemical soil properties in the 0–30 cm soil layer. Values present mean ± standard error.

Soil properties	Mean ± SE
Clay (%)	9.8 ± 1.7
Silt (%)	83.8 ± 4.3
Sand (%)	6.4 ± 6.0
Bulk density (g cm^{-3})	1.13 ± 0.19
pH	5.8 ± 0.5
C (%)	1.8 ± 0.6
N (%)	0.15 ± 0.06
Carbon stock (t/ha)	56.9 ± 3.0
C:N	11.4 ± 0.2

by silt (Fig. S9).

3.2. Cabbage harvest

There were no significant differences in the mean total biomass or water content in the cabbage heads and roots when comparing inside and outside of the chamber (all $p > 0.2376$), however, the water content of the leaves inside the chambers was significantly higher (inside: 72.2 ± 0.4; outside: 65.7 ± 2.0; t(5.4) = 3.2, p = 0.0221, Cohen's d= 1.8; Fig. 4a and b, Table S2). Furthermore, total C concentrations were significantly higher in cabbage leaves and cabbage heads outside the chambers (leaves: outside: 38.6 ± 0.3; inside 36.3 ± 0.2; t(8.4) = −6.3; $p > 0.001$, cabbage heads: outside: 39.4 ± 0.2; inside: 38.3 ± 0.3; t (8.8) = −2.7; p = 0.025; Cohen's d= −1.6), while total N content was significantly higher for leaves, roots, cabbage inside chamber (all $p < 0.0327$; Table S3, Fig. 4c and d). C:N was significantly higher outside chambers for cabbage and leaves (all $p < 0.0111$; Table S3; Fig. 4e).

3.3. N_2O and CH_4 emissions

Emissions from chambers containing cabbage consistently exceeded the N_2O emissions from the fallow chambers (Fig. 5a). The highest daily mean flux measured was 682 μg N m^{-2} h^{-1} for cabbage on 17 November 2024, while the highest flux for fallow was 55 μg N m^{-2} h^{-1} (on the same day). Mean emissions for the entire study period were significantly higher under cabbage than fallow (104 ± 140 and 15.3 ± 11.2 μg N m^{-2} h^{-1}, respectively (t (2.01)= 10.85; p = 0.008; Cohen's d= 8.86; Table S4; Fig. S10).

Using a linear mixed-effects model confirmed that treatment had a significant effect on N_2O fluxes (p = 0.021, Marginal R^2=0.242, Table S5). There was also a significant interaction between treatment and time (p = 0.011), indicating that the temporal pattern differed between treatments, with fluxes under cabbage declining more steeply over time than under fallow.

Emissions in cabbage varied over time, with 72% of total N_2O emissions emitted between 06 November 2024 and 26 November 2024, which equals 27% of the observational period. In the same period, the fallow land use experienced a peak in emissions as well and emitted 47% of its total emissions. All days between 09 November 2024 and 20 November 2024 were classified as hot moments for the cabbage, while fluxes for fallow was only considered a hot moment one day (17 November 2024). In the beginning of December another smaller peak was observed in the cabbage, but it was too low to be identified as hot moment.

The highest daily mean CH_4 emission recorded was 919 μg C m^{-2} h^{-1} from start November and noted for cabbage (Fig. 5b). The highest emission from the fallow was 615 μg C m^{-2} h^{-1} (01 November 2024). The emission trends followed each other between the two land uses and differences were not significant (Fig. 5b). Mean emission for the entire period were not significantly different (Cabbage: 30.04 ± 4.66; Fallow: 18.58 ± 7.69; t (3.3) = 1.3; p = 0.285; Cohen's d= 1.0; Table S6).

Daily emissions of CH_4 vary markedly over time, with 56% and 65% of daily emissions being negative for cabbage and fallow, respectively (not below −64.6 μg C m^{-2} h^{-1}).

Measurements for N_2O did not differ significantly within the same treatment across the three replicates ($p > 0.2$), while there were significant differences for CH_4 within the same treatment (cabbage: p = 0.029; fallow: $p < 0.001$; Table S8). There were no significant differences for clear and dark measurements (Fig. S11; Table S7).

The combination of cabbage and fertilizer has an influence on N_2O but not CH_4 when compared to fallow.

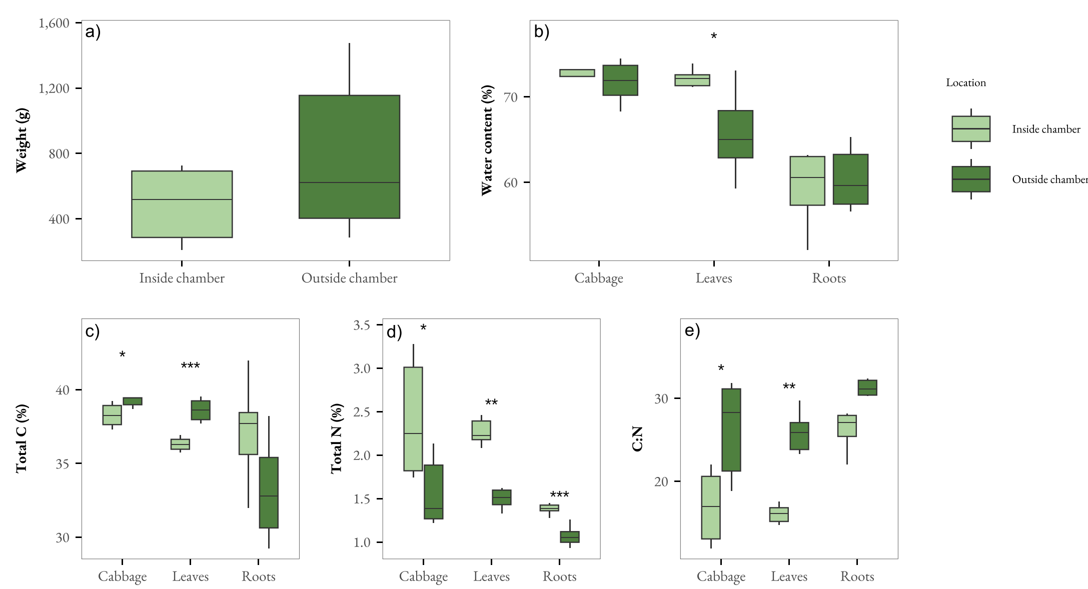

Fig. 4. **a)** Box plots of fresh weight after washing of the whole cabbage plant, divided into inside and outside chambers grown cabbages (n = 6). **b)** Water content of inside and outside grown cabbages divided into the fractions cabbage, leaves, and roots. Asterisks indicate statistically significant differences between groups (n = 6). **c), d), and e)**: Box plots of total C (%), N (%), and C:N from inside and outside grown cabbages, divided into the fraction cabbage, leaves, and roots (n = 6). Asterix indicate statistically significant differences between groups (n = 6).

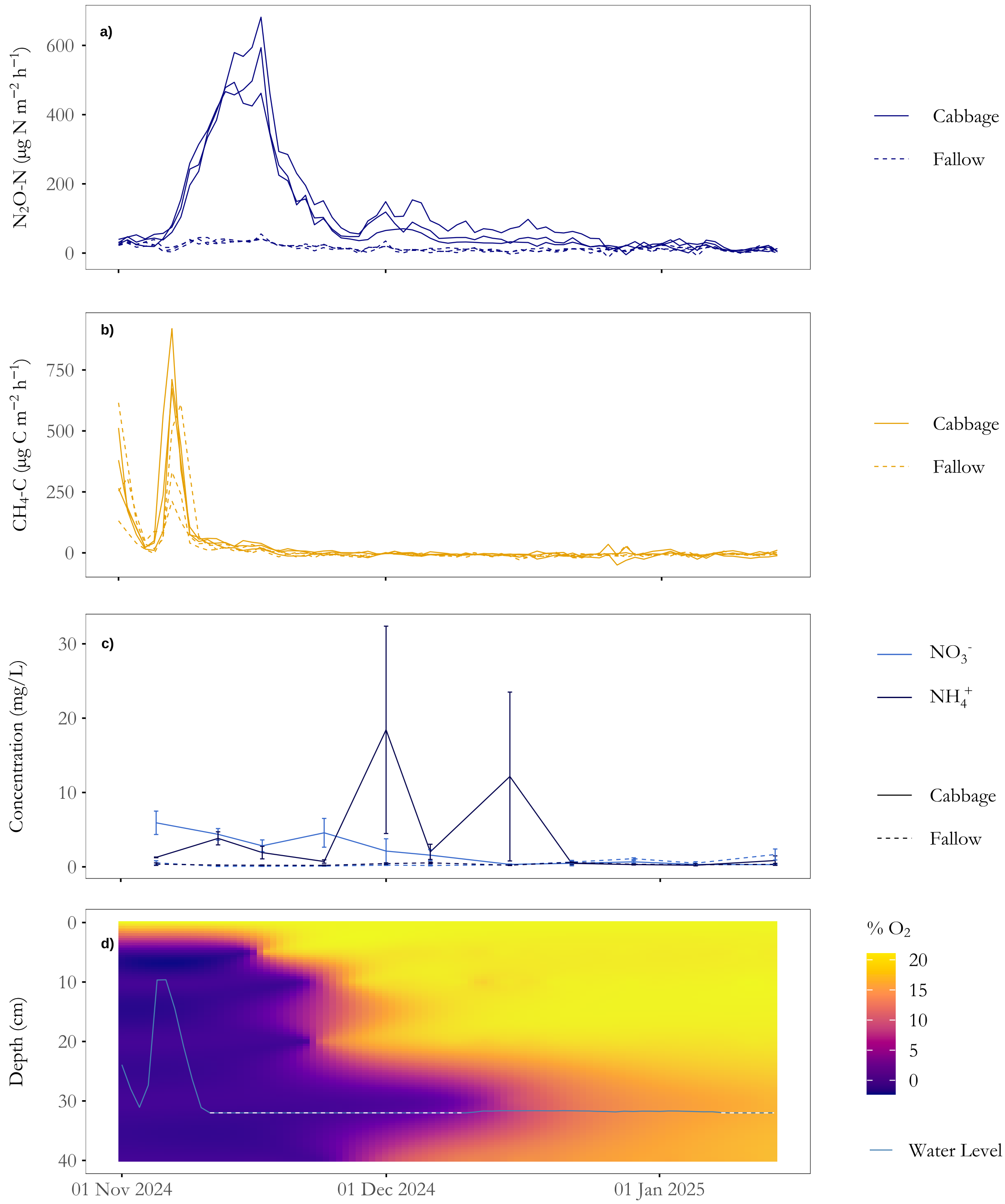

Fig. 5. Daily mean (n = 3) emissions of N_2O **a)** and CH_4 **b)** (µg N m^{-2} h^{-1} and µg C m^{-2} h^{-1}) over the experimental period 01 November 2024–14 January 2025. Emissions from chambers containing cabbage that received fertilizer (bold line), and emissions from the fallow chambers (dashed line) **c)** mean concentration of soil extracted NH_4^+ and NO_3^- for cabbage and fallow at depth 0–2 cm (n = 3) and 13–15 cm (n = 3). **d)** oxygen levels at different depths overlayed with the water table (water tables below 32 cm are marked with a dashed line). Measured values are from depths 2.5, 5, 10, 20, 30, and 40 cm combined with atmospheric O_2 at 0 cm, while values in between are interpolated.

3.4. Soil oxygen

Soil oxygen concentrations increased throughout the study period after the drop in water table and fastest in layers close to the surface (Fig. 5d, Fig. S12). In 5 cm depth, O_2 reached 50% of atmospheric saturation by 16 November 2024 and 80% by 18 November 2024. At 20 cm, this was delayed, where 50% saturation was reached on 24 December 2024 and 80% on 29 December 2024. The sensor at 30 cm showed the slowest response, reaching 50% saturation on 17 December 2024 and 80% on 11 January 2025.

3.5. NO_3^- and NH_4^+

The concentrations of NO_3^- differed between cabbage and fallow plots in their raw means, with higher values in cabbage plots (2.14 ± 2.02 L^{-1}) compared to fallow plots (0.491 ± 0.498 mg L^{-1}) (Fig. 5c and S13). This difference was however, not significant as a main effect in the linear mixed model ($p = 0.160$, R^2=0.631 Table S9). NO_3^- concentrations were strongly influenced by significant Treatment × Depths × Time interactions ($p < 0.001$), indicating that the treatment effect varied depending on both soil depth and sampling date.

Concentrations were significantly higher in the top (0–2 cm) soil layers compared to the bottom (13–15 cm) soil layers with a significant interaction between treatment and depths ($p < 0.001$).

Concentrations of NH_4^+ did not differ significantly between cabbage and fallow with mean concentrations of 3.84 (±5.93) mg L^{-1} and 0.343 (±0.133) mg L^{-1} respectively ($p = 0.914$), as well as there were no significant differences between the two measured depths (Fig. S13; $p = 0.643$, Table S10).

Concentrations changed significantly over time for NO_3^-, but not for NH_4^+($p < 0.001$ and $p = 0.643$, respectively).

NO_3^- levels in cabbage plots decreased over time (with the exception 24 November 2024), while cabbage NH_4^+ concentration fluctuated more. Fallow NH_4^+ and NO_3^- concentrations remained low and showed no systematic temporal trend.

Mean pH levels throughout the period ranged from 5.5 to 7.3 with significant differences between depths but not between cabbage and fallow plots ($p < 0.001$ and $p = 0.066$, respectively, Table S11). A general increase for pH was noted over time (Fig. S14a).

3.6. LandscapeDNDC

Following the last rainfall event on 05 November 2024 and the onset of field drainage, the use of site-specific van Genuchten parameters (α and n) in the first step of our three-step approach enabled LandscapeDNDC to accurately simulate the decline in soil water content across soil depths of 5–40 cm (Fig. 6). Model performance was high, with R^2 values ranging from 0.53 to 0.81, mean RMSE between 3.1 – 6.1 vol%. Only the measured soil water content at 2.5 cm was less accurately represented. While the simulations showed a similar pattern at 2.5 and 5 cm soil depth due to identical hydrologic properties, the measured content was considerably higher at 2.5 cm than at 5 cm.

The default value of 2.333 for the physical soil gas diffusivity parameter Ω_{MDEEA} resulted in an overly rapid increase in simulated O_2 partial pressure at 5 cm soil depth (Fig. 6). Consequently, the simulated peak nitrous oxide (N_2O) emissions occurred at an earlier time point as compared to the measurements. In the second step, constraining Ω_{MDEEA} to a higher value of 4.42 improved the fit to measured O_2 (R^2: 0.66–0.93, RMSE: 2.1–4.4%; Table S15). However, this adjustment also strongly reduced the simulated N_2O emissions peak and the accumulated emission during the measurement period from formerly 1.33–0.55 N ha^{-1}.

In the final step, constraining the (de)nitrification parameters yielded a simulated N_2O peak that closely matched the measurements (Fig. 6 and S15). In the best-fitting parameter set, the peak N_2O emissions were predominantly associated with denitrification, while the subsequent tail of N_2O emissions was mainly related to nitrification. Integrating over the entire measurement period resulted in a median contribution of 43 ± 20% from denitrification and 57 ± 20% from nitrification to total N_2O production. The corresponding parameter distributions are provided (Fig. S16).

3.7. N_2O and CH_4 budgets, GWP, and emission factor

The cumulated total N_2O emissions across the observational period were 187.9 ± 14.6 mg N m^{-2} for the chambers with cabbages and 27.5 ± 0.7 mg N m^{-2} for the fallow chambers ($n = 3$) (Fig. 7a; Table S13), equal to a 7-fold increase in fluxes in cabbage treatment compared to fallow. For CH_4, the cabbage emitted 54.1 ± 8.4 mg C m^{-2}, while the fallow emitted 33.5 ± 13.8 mg C m^{-2}, which equals a factor of 1.6 between the two land uses.

The highest GWP for the experimental period originated from the cabbage chambers with N_2O emissions having a higher GWP than CH_4 for both land uses. N_2O emissions from cabbage correspond to 80.6 ± 6.3 g m^{-2} CO_2-eq, while emissions from fallow correspond to 11.8 ± 0.3 g m^{-2} CO_2-eq. Emissions from CH_4 correspond to 2.0 ± 0.3 and 1.2 ± 0.5 g m^{-2} CO_2-eq for cabbage and fallow, respectively (Fig. 7b).

The N equivalent N_2O emission were 187.9 ± 14.6 mg N m^{-2} and 27.5 ± 0.7 mg N m^{-2} for cabbage and fallow, respectively. Compared with the N input throughout the season, this corresponds to an EF of 0.52% when looking at total emissions until 25 December 2024 (only including the first fertilization of 300 kg N ha^{-1}) and an EF of 0.26% until 10 January 2025 (including 600 kg N ha^{-1}). The last fertilization is not included in these EF's as it was applied only four days prior to the harvest where emissions were very low.

Cabbage plants from both inside and outside chambers produced a yield of 1315.87 kg dry biomass ha^{-1} (whole plant, including roots).

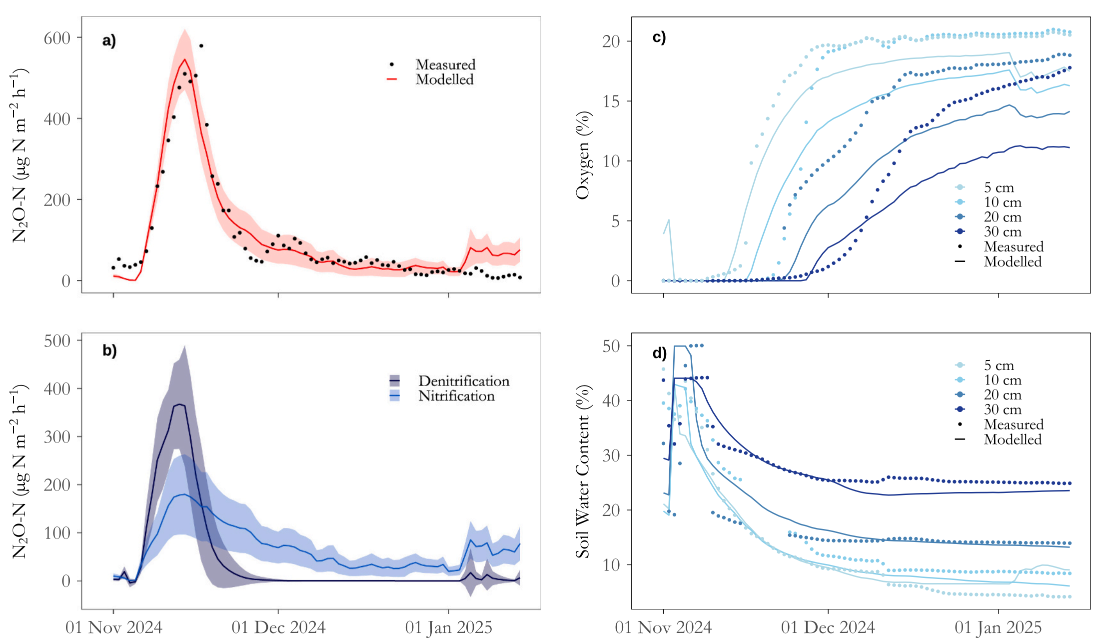

Fig. 6. a) Measurements from cabbage chambers (black dots) and LandscapeDNDC modelled emissions (red line) of N_2O in µg N m^{-2} h^{-1}, modelled SD is indicated by red shading b) Fluxes (µg N m^{-2} h^{-1}) of net N_2O production from nitrification and denitrification modelled with LandscapeDNDC, SD is indicated by shading. c) Measured (dots) and modelled (bold line) concentration of oxygen (%) at depths 5, 10, 20, and 30 cm, represented by a blue colour scale. d) Measured (dots) and modelled (bold line) volumetric soil water contents at depths 5, 10, 20, and 30 cm.

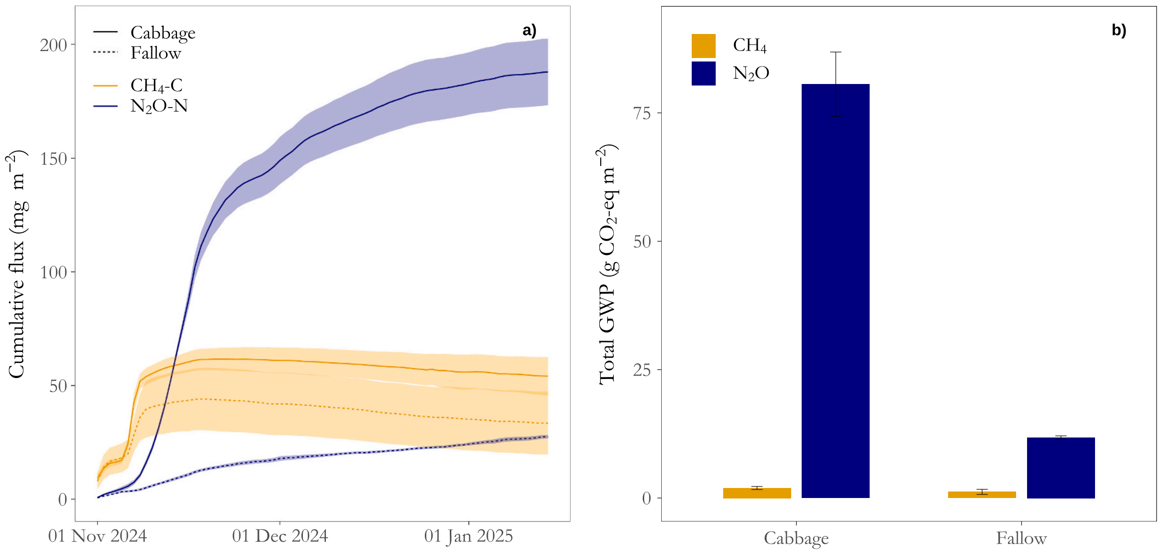

Fig. 7. a) Total emissions of N_2O (blue, mg N m^{-2}) and CH_4 (orange, mg C m^{-2}) for cabbage and fallow seasons, including error bars showing the standard deviation (n = 3). **b)** Total emissions for N_2O (blue) and CH_4 (yellow) in CO_2-equivalents for cabbage and fallow (n = 3).

When applying the mean N content of 1.72%, this equals 226.2 N ha^{-1}, which corresponds to a NUE of 38% with the input of 600 N ha^{-1} or a NUE of 25.1% when including the last fertilization (total of 900 N ha^{-1}). When looking only at chamber-plants, the NUE reaches 44.3% with 600 N ha^{-1} and 29.5% with 900 N ha^{-1}. Note that the NUE values are not considering the initial soil nitrogen, as the reactive nitrogen was not measured previously. However, N levels above the hardpan were 0.15% (fig. S8).

4. Discussion

This study has shown unprecedented temporal resolution measurements of CH_4 and N_2O fluxes using automated chambers over a fallow period and a cabbage-growing season in a subtropical rice-vegetable rotation system. Furthermore, we have presented subsurface O_2 measurements to constrain the process attribution using LandscapeDNDC in a real-field Vietnamese management context.

4.1. Emission patterns

There are clear temporal and magnitude-based differences in emission patterns between cabbage cultivation and fallow land and N_2O and CH_4. N_2O emissions from fertilized cabbage plots exceeded those from fallow significantly, while CH_4 emissions did not. This indicates that N_2O emissions are strongly influenced by the effect of cabbage cultivation, whereas CH_4 emissions remain unaffected. Furthermore, both N_2O and CH_4 emissions vary strongly throughout the season. While CH_4 has brief periods with high emissions (narrow peaks, start November), N_2O emissions peak over a 20-day period in November when 72% of the total N_2O emissions took place. In terms of magnitude, the daily mean N_2O emission for this cabbage season is approximately 104 μg N m^{-2} h^{-1} with the highest daily mean flux being 682 μg N m^{-2} h^{-1}. This lies within the range of reported values, though on the higher end, when looking at maximum emissions of upland cabbage in higher latitudes (Fan et al., 2022; Jhang et al., 2022; Pang et al., 2009). Total seasonal emissions of 1.88 kg N_2O-N ha^{-1} are well within the range reported in a meta study by Rezaei Rashti et al. (2015), although this study's cabbage season was rather short. Fallow emissions peak with 55.4 μg N m^{-2} h^{-1} and a mean emission of 15.3 μg N m^{-2} h^{-1}. Compared to other studies, this study's fallow emissions are higher or similar (Li et al., 2021; Xu et al., 2022). However, Ju et al. (2024) measured N_2O emissions in fallow seasons with different rates of N fertilization over three years and found emission rates with maximum values in a range of 20.1–583.4 g N_2O-N ha^{-1} day^{-1}, whereas this study measured a maximum emission of 13.3 g N_2O-N ha^{-1} day^{-1}.

The fact that hot moments have been identified and that they dominate the N_2O fluxes, emphasizes the advantage of high-resolution measurements used in this study. Weekly or bi-weekly manual chamber measurements are likely to have underestimated the magnitude or duration of the hot moment. Even though this study measured with high temporal resolution, only the daily means are shown.

4.2. Environmental drivers

This study quantifies greenhouse gas emissions for cabbage in combination with fertilizer because that is the normal management practice in rice paddies in North Vietnam. It is therefore impossible in this study to separate the effect of cabbage as a crop type and the fertilization application as compared to fallow.

N fertilizer is linked to N_2O emissions, as it provides substrates for both nitrification and denitrification (Liao et al., 2021). As mentioned earlier, several factors such as timing, concentration, and application methods are relevant. NO_3^- and NH_4^+ levels were higher in cabbage plots than fallow plots, indicating that the fertilization is the primary source for N_2O emissions. The hot moment began one day after the first fertilization, as indicated by an increase in NH_4^+ concentration in the soil, which decreased briefly after. NO_3^- concentrations increased by 24 November 2024, which likely reflects nitrification activity producing NO_3^-, while the decrease may be due to denitrification, which consumes NO_3^-. Together with the large N_2O emission peak, this suggests that a large proportion of the emissions was due to nitrification and denitrification, which a few days later was reflected by the increased concentrations of NO_3^- in the soil. This hypothesis is supported by the LandscapeDNDC model, which also predicts a high nitrification rate (Fig. 6). The nitrification peak in the model output is more prolonged (more tailing) than the N_2O emission peak, suggesting the higher oxygen levels later in the season may have favoured complete oxidation of NH_2OH, thereby reduced N_2O produced from nitrification. Furthermore, because NO_3^- is at risk of leaching and only the plots containing cabbage received fertilizer and were irrigated, it is possible that NO_3^- leached away from these plots into other areas of the field (Wang et al., 2019).

The LandscapeDNDC model was also applied to explore the sensitivity of different levels of N fertilizer input on the corresponding N_2O emissions (Fig. 8). It is noted that N_2O emissions reach a plateau after

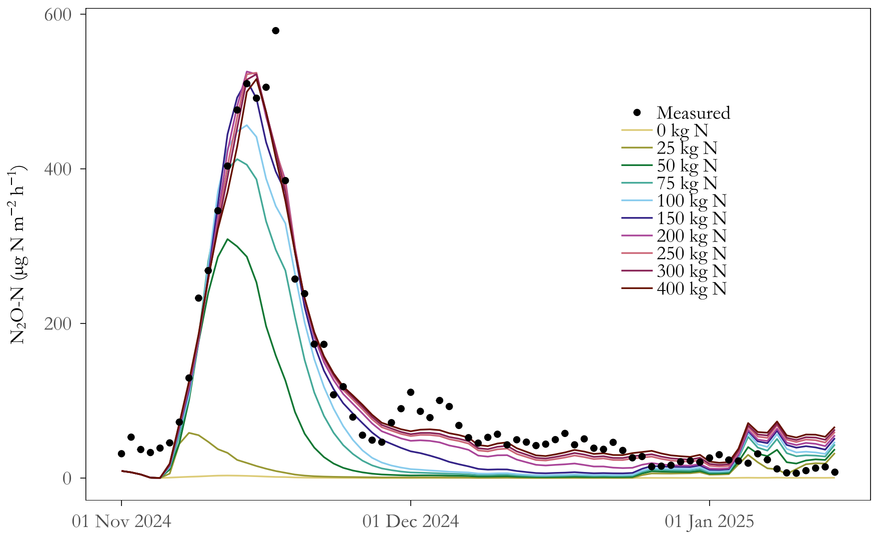

Fig. 8. N_2O emissions (kg N ha^{-1} day^{-1}) with different rates of N fertilizer per fertilizing event. Actual fertilizing was approximately 300 kg N ha^{-1} per fertilizing event.

approximately 200–300 kg N ha^{-1}. This suggests that the microbial nitrification capacity is reached and other environmental drivers than N availability are constraining additional N_2O emissions. Lack of bioavailable dissolved carbon could be one candidate, but this cannot be confirmed by our observations. A substantial reduction in N_2O emissions was observed at e.g. 50 kg N ha^{-1}, highlighting the potential of reducing future N_2O emissions by reducing the N inputs.

The cabbage plant itself may also influence N_2O emissions. Its roots consume oxygen, creating low-oxygen environments, which may promote denitrification (Burgin and Groffman, 2012; Woldendorp, 1962). Furthermore, they release organic compounds that can stimulate microbial activity in general by providing energy sources (Rumeau et al., 2025).

4.3. N_2O emission factor, N efficiency and GWP

A total nitrogen application of approximately 900 kg N ha^{-1} during the cabbage season resulted in cumulative N_2O emissions of 187.9 ± 14.6 mg N m^{-2}. This corresponds to an EF of 0.52%, which is within the range for EFs from paddy rice fields with multiple drainage (Intergovernmental Panel On Climate Change Ipcc, 2019). However, studies with upland cabbage reported higher EFs (Jhang et al., 2022). The N fertilizer application rate in this study is in the high end compared to other studies, which also affects the EF (Brito et al., 2012; Cao et al., 2023). The NUE of 38% falls at the lower end of reported values, indicating suboptimal N uptake or fertilizer overapplication (Ladha et al., 2005; Raun and Johnson, 1999). Cao et al. (2023) found an optimal N fertilizer rate of 250 kg N ha^{-1} per growing season for achieving the highest yield of Chinese cabbage when testing application rates ranging from 0 to 450 kg N ha^{-1}. Above 250 kg N ha^{-1}, yields started to plateau. Other studies report similar results for different cabbage species (Kacjan Maršić et al., 2021; Robinson, 2020). Likely this study reached a plateau, explaining the low NUE. It is important to note that both EF and NUE are obtained under a high fertilization regime and may not be generalized to lower, more realistic rates. Many farmers overfertilize their crops; a survey from Cao et al. (2023) with 52 farmers from southwest China found that the mean fertilization rate for vegetables is 450 kg N ha^{-1}. Such practices are not economically favorable and have adverse effects, including increased N_2O emissions, NO_3^- leaching, and NH_3 volatilization.

Due to the shortened growing season, it is challenging to draw definitive conclusions regarding cabbage yield. Assuming upscaling of the experimental plots to a hectare scale (bearing in mind that cabbage in paddy soils typically is grown on elongated "islands" surrounded by water, limiting the usable area, the estimated yield is approximately 13.15 tons dry biomass ha^{-1} (based on 2 plants per 0.31 m^2, equaling the chamber area). Subtracting plant uptake and N_2O emissions (using the EF) from the total applied N, close to 25% of the applied N was lost to other sources, which were not further investigated in this study. Potential pathways include NH_3 volatilization, N_2 emissions from complete denitrification and leaching of NO_3^- (Schwenke, 2022). Lee et al. (2024) finds NH_3 volatilization rates from cabbage grown in upland fields to range from 2.6% to 4.7%, and 10.2 to 10.8% from flooded paddy soils. Ma et al. (2021) found that vegetables can lose up to 15% of N input through NH_3 volatilization and that volatilization does not increase linear with the N input (Lee et al., 2024). Ammonium ions (NH_4^+) are in equilibrium with NH_3 molecules, and the proportion of NH_3 increases when pH is $>$ 7, which leads to greater volatilization (Schwenke, 2022). NH_3 contributes to air pollution and poses harmful effects to both human health and the environment (Williams, 2022). Due to the presence of a hardpan in paddy fields, NO_3^- leaching is limited, because water infiltration into deeper soil levels is limited (Chen and Liu, 2002). During fallow and cabbage-growing seasons, bunds around paddy rice field are typically open to allow free drainage, which also means that NO_3^- can freely be released to the environment. When aerobic conditions limit denitrification, as it was the case in this study, NO_3^- can accumulate. When the field is reflooded for the rice season, this NO_3^- can become available for denitrification, producing substantial amounts of N_2O. This suggests that fertilization from a vegetable season might have adverse environmental effects during the next rice season. These adverse pathways, including N_2O emissions, further highlight the need of optimizing N inputs.

When examining GWPs for both GHGs for both land uses, N_2O was the dominant contributor during this non flooded season. Furthermore, N_2O emissions were a factor seven higher from cabbage cultivation than fallow. The N_2O emissions from fallow use were lower than cabbage, though when expressed in CO_2-eq of N_2O, they also exceed those of CH_4. Ju et al. (2024) compared N_2O emissions from a rice season to a fallow season and found the majority of N_2O emissions to occur during the fallow season, highlighting the importance of accounting for N_2O emissions in all land uses. Typical CO_2-eq from rice seasons are reported at 21–173 g m^{-2} for CH_4 and −5 (indicating uptake) to 12 g m^{-2} for N_2O (Adviento-Borbe and Linquist, 2016; Li et al., 2011; Ma et al., 2013). While the total GWP for a rice season exceeds those of cabbage and fallow it remains essential to consider annual land uses. From this study we can conclude that N_2O emissions are significantly higher when growing fertilized cabbage compared to emissions from fallow land, while CH_4 emissions did not differ significantly between the two land uses. Both land uses still emit substantial amounts of GHGs and should be included in any comprehensive annual GHG budget for paddy soils.

4.4. Limitations

The setup in this study is made to reflect two contrasting but realistic land uses (cabbage + fertiliser versus untreated fallow), but we note that a full factorial design would have been a stronger setup to strengthen interpretation of differences in fluxes. For future investigations it would further be relevant to assess to what extent cabbage growth inside the chambers can be biased given that conditions inside chambers differ slightly from those outside and do not exactly correspond to the cultivation technique. When comparing cabbages inside and outside the chambers, no significant differences were found in weight and water content (except for the leaf fraction), suggesting growth conditions did not vary markedly. However, C and N content differed significantly for all plant parts between cabbages inside and outside the chambers.

The chambers in this study are placed quite close to each other, to allow the cables to reach the analyzers. This limits the spatial resolution of emissions. However, the paddy soil in the field appeared relatively homogeneous, and the two treatments (cabbage and fallow) did not differ significantly within their respective land use. An approach presented by e.g. Tariq et al. (2022), is the use of automatic chambers in the combination of manual chambers, which could be further investigated.

The applied nitrogen N rate for cabbage treatments largely exceeds published optima for cabbage. Both the emission factor (0.52%) and nitrogen-use efficiency (38%) were obtained under over-fertilization conditions and may not be representative of normal farmer practice or lower-rate scenarios.

Additionally, the cabbage growing season was rather short and occurred under drier-than-average conditions (only 18.9 mm rain in November–December vs long-term average). Results may differ substantially in wetter years or with a full-length cabbage crop.

The study was conducted at a single site during one season only. Generalization to the broader Red River Delta or other rice–vegetable rotations requires caution; landscape-scale replication and multi-year data are needed before strong policy recommendations can be made.

5. Perspectives and conclusions

5.1. Conclusions

This study's major strengths lie in its high-resolution dataset, direct linkage of O_2 dynamics to N_2O pathways, and demonstration that non-rice phases can dominate annual N_2O budgets in paddy systems -findings that were made possible by continuous field measurements combined with process-based simulations. We conclude that N_2O emissions from cabbage cultivation under fertilization exceed those from fallow land by a factor of seven, while CH_4 emissions showed no significant differences between the two land uses. Furthermore, N_2O emissions outweigh those from CH_4 when measured as CO_2-equivalents, emphasizing the importance of focusing on N_2O emissions, particularly during dry seasons in paddy soils. Notably, a period of 12 days was identified as a hot moment, in which the majority of the total N_2O emissions was emitted. This highlights the importance of using automatic chambers, as manual static chambers are likely to underestimate the full magnitude of N_2O emissions during such a hot moment, which in our case followed a few days after fertilization and a rain event. Model results suggest that denitrification, followed by nitrification, were the dominant processes producing N_2O. This was supported by measurements of NO_3^- and NH_4^+ concentrations as well as O_2 dynamics. Finally, sensitivity analyses using LandscapeDNDC suggest that N_2O emissions plateau at application rates above approximately 200–300 kg N ha^{-1}. This indicates that a maximum nitrification rate has been reached.

5.2. Perspectives

N_2O emissions are important for most GHG budgets associated with agriculture, and a key target for mitigation efforts. Various strategies have been explored to reduce emissions including adjustments of fertilization amount, timing, and placement. Many farmers overfertilize crops, and reducing N fertilizer can markedly reduce N_2O emissions, as modelled by LandscapeDNDC (Fig. 8). Additionally, fertilizer amount has several adverse effects beyond increased N_2O emissions, such as NO_3^- leaching and NH_3 volatilization. Furthermore, fertilizers are an investment, and when crop yields do not increase beyond a certain fertilization rate, applying excess fertilizer is no longer economically favourable. One promising approach is split applications, which may increase the amount of NH_4^+ taken up by plants per fertilization event (Sajjad et al., 2024). This means fewer residual N compounds that are available for nitrification and denitrification, reducing N_2O emissions.

In addition to management practices, technological innovations could play a vital role. In this study, the only hot moments were captured in combination with a rainfall event. Sensor informed or weather responsive approaches for timing fertilization could help avoid high N_2O emissions during such events. Precision application, which is a practice where the fertilizer is applied below the surface, has also gained increasing attention. This technique minimizes surface-level microbial activity, thereby reducing nitrification and denitrification, while also increasing plant uptake since nutrients are closer to the roots. Other promising approaches for reducing both N_2O emissions and NO_3^- leaching, include nitrification inhibitors, slow-release fertilizers, and biochar application (Dong et al., 2021; Tariq et al., 2022; Trinh et al., 2017; Yi et al., 2023). Residue management practices, such as incorporation or removal of crop residues, also influence soil N dynamics and emissions (Nguyen et al., 2016). Additionally, carry-over effect of residual nitrate from vegetable season that persist phase into the subsequent flooding season should be quantified, as they are likely to be overlooked due to neither being the vegetable season nor the rice season.

Mitigation strategies for paddy rice cultivation are complex, particularly due to the need of balancing different GHGs. Approaches such as AWD, which involve single or multiple drainage, are increasingly promoted due to their very effective inhibition of CH_4 emissions. However, as observed in a few studies, this may have adverse effects on N_2O emissions (Zhao et al., 2024). Especially the transitions between wet and dry conditions can create ideal conditions for both nitrification and denitrification, which also has been observed in this study. In addition to technical considerations, climate change complicates water management strategies further. As climate change alters rainfall intensity and temperature patterns, it has significant implications not only for rice production but also associated with GHG emissions themselves. Studies have found certain climate change-driven conditions can lead to the production of both N_2O and CH_4, indicating that the emissions may reinforce themselves through positive feedback loops (Intergovernmental Panel On Climate Change Ipcc, 2021). Climate change connected water scarcity would promote implementation approaches that reduce flooding of rice paddies, potentially shifting the GHG emission balance even further.

Current knowledge of N_2O dynamics in paddy soil is limited, partly due to the widespread use of manual static chambers, which likely miss hot moments. More high-resolution monitoring is needed to understand temporal and spatial variability of N_2O emissions. Furthermore, it would be of high interest to investigate to what degree findings from this study can be upscaled across larger regions, such as RRD. Factors that need to be considered include land use, climatic conditions, and soil properties. Policy makers need to recognize the role of fallow and vegetable periods in the total GHG budget of rice paddies, instead of solely focusing on rice cultivation. It would be of high value to shift a rice-centric view to considering the whole annual cropping cycle of paddy soils. Taking this study's findings into account, this study highlights the importance of

GHG emissions from paddy soils outside the main rice seasons, and that future remediation actions should include high-resolution N_2O monitoring and process-based modelling of both rice and non-rice phases when constructing annual GHG budgets for rice-vegetable rotations.

CRediT authorship contribution statement

Lara Melissa Fritzsche: Writing – original draft, Visualization, Methodology, Investigation, Formal analysis, Data curation, Conceptualization. **Hans Frederik Engvej Hansen:** Writing – review & editing, Validation, Supervision, Methodology, Data curation, Conceptualization. **David Kraus:** Writing – review & editing, Visualization, Validation, Methodology, Data curation. **Marija Popovic:** Investigation, Formal analysis, Data curation. **Rosa Elvira Hvidsten Gregersen:** Investigation, Formal analysis, Data curation. **Klaus Steenberg Larsen:** Writing – review & editing, Validation, Methodology. **Vu Duong Quynh:** Supervision, Methodology, Conceptualization. **Mai Van Trinh:** Writing – review & editing, Methodology, Conceptualization. **Nguyen Thi Oanh:** Methodology, Investigation, Data curation. **Bo Elberling:** Writing – review & editing, Supervision, Project administration, Methodology, Investigation, Conceptualization.

Declaration of Generative AI and AI-assisted technologies in the manuscript preparation process

During the preparation of this work, the author used ChatGPT (OpenAI) to assist with code debugging, checking calculations, structuring the manuscript, and brainstorming ideas. All outputs generated by this tool were reviewed, verified, and edited by the authors, who takes full responsibility for the content, analyses, and conclusions presented in the published article.

Declaration of Competing Interest

The authors declare that they have no known competing financial interests or personal relationships that could have appeared to influence the work reported in this paper.

Acknowledgements

Many thanks to Allan Olesen and Henrik Christensen for help with setting up, calibrating, and maintaining machinery at the field site, to Nguyen Trong Thanh for being responsible and very helpful at our experiment site and to lab technicians Søs Marianne Ludvigsen, Maja Holm Wahlgren, and Steen Færgemann Hansen for analyzing soil, water and gas samples. Thanks to Hay for translating, Niklas, Anna, Sophie and Sara for helping in the field. The study was funded by Novo Nordisk Foundation through the Global Wetland Center (research grant NNF23OC0081089), partly funded by IAEA through project CRP D.1.50.20, and Niels Kingo Jacobsen Travel scholarship.

Appendix A. Supporting information

Supplementary data associated with this article can be found in the online version at doi:10.1016/j.agee.2026.110623.

Data availability

Research Link Provided.

emissions and soil measurements (ERDA (Electronic research data archive, University of Copenhagen))

References

Adviento-Borbe, M.A.A., Linquist, B., 2016. Assessing fertilizer N placement on CH4 and N2O emissions in irrigated rice systems. Geoderma 266, 40–45. https://doi.org/10.1016/j.geoderma.2015.11.034.

Akiyama, H., Yagi, K., Yan, X., 2005. Direct N_2 O emissions from rice paddy fields: summary of available data. Glob. Biogeochem. Cycles 19 (1). https://doi.org/10.1029/2004GB002378.

Barton, L., Wolf, B., Rowlings, D., Scheer, C., Kiese, R., Grace, P., Stefanova, K., Butterbach-Bahl, K., 2015. Sampling frequency affects estimates of annual nitrous oxide fluxes. Sci. Rep. 5 (1). https://doi.org/10.1038/srep15912.

Bates, D., Mächler, M., Bolker, B., Walker, S., 2015. Fitting linear mixed-effects models using lme4. J. Stat. Softw. 67 (1). https://doi.org/10.18637/jss.v067.i01.

Beck, H.E., McVicar, T.R., Vergopolan, N., Berg, A., Lutsko, N.J., Dufour, A., Zeng, Z., Jiang, X., Van Dijk, A.I.J.M., Miralles, D.G., 2023. High-resolution (1 km) Köppen-Geiger maps for 1901–2099 based on constrained CMIP6 projections. Sci. Data 10 (1). https://doi.org/10.1038/s41597-023-02549-6.

Bernhard, A., 2010. The nitrogen cycle: processes, players, and human impact. Nat. Educ. Knowl. 3 (10). ⟨https://www.nature.com/scitable/knowledge/library/the-nitrogen-cycle-processes-players-and-human-15644632/⟩.

Bollmann, A., Conrad, R., 1998. Influence of O_2 availability on NO and N_2 O release by nitrification and denitrification in soils. Glob. Change Biol. 4 (4). https://doi.org/10.1046/j.1365-2486.1998.00161.x.

Bouman, B.A.M., Tuong, T.P., 2001. Field water management to save water and increase its productivity in irrigated lowland rice. Agric. Water Manag. 49 (1). https://doi.org/10.1016/S0378-3774(00)00128-1.

Brito, L.M., Amaro, A.L., Mourão, I., Moura, L., 2012. Yield and nitrogen uptake of white cabbage (Brassica oleracea var. Capitata) with organic and inorganic fertilisers. Acta Hortic. (933). https://doi.org/10.17660/ActaHortic.2012.933.11.

Burgin, A.J., Groffman, P.M., 2012. Soil O_2 controls denitrification rates and N_2 O yield in a riparian wetland. J. Geophys. Res. Biogeosci. 117 (G1). https://doi.org/10.1029/2011JG001799.

Cao, H., Zhang, F., Fu, J., Ma, X., Wang, J., Liu, F., Guo, G., Tian, Y., Liang, T., Zhou, N., Wang, Y., Chen, X., Wang, X., 2023. Optimized nitrogen fertilizer rate can increase yield and nitrogen use efficiency for open-field Chinese cabbage in Southwest China. Agronomy 13 (6). https://doi.org/10.3390/agronomy13061578.

Chen, S.-K., Liu, C.W., 2002. Analysis of water movement in paddy rice fields (I) experimental studies. Article 1–4. J. Hydrol. 260 (1–4). https://doi.org/10.1016/S0022-1694(01)00615-1.

Christiansen, J.R., Outhwaite, J., Smukler, S.M., 2015. Comparison of CO2, CH4 and N2O soil-atmosphere exchange measured in static chambers with cavity ring-down spectroscopy and gas chromatography. Agric. For. Meteorol. 211–212, 48–57. https://doi.org/10.1016/j.agrformet.2015.06.004.

Conrad, R., 2007. Microbial Ecology of Methanogens and Methanotrophs. In: Advances in Agronomy, 96. Elsevier, pp. 1–63. https://doi.org/10.1016/S0065-2113(07)96005-8.

Dong, D., Li, J., Ying, S., Wu, J., Han, X., Teng, Y., Zhou, M., Ren, Y., Jiang, P., 2021. Mitigation of methane emission in a rice paddy field amended with biochar-based slow-release fertilizer. Sci. Total. Environ. 792, 148460. https://doi.org/10.1016/j.scitotenv.2021.148460.

Fan, D., Wang, X., Song, D., Shi, Y., Chen, Y., Wang, J., Cao, B., Zou, G., He, W., 2022. Optimizing nitrogen management to mitigate gaseous losses and improve net benefits of an open-field Chinese cabbage system. J. Environ. Manag. 318, 115583. https://doi.org/10.1016/j.jenvman.2022.115583.

Food and Agriculture Organization of the United Nations. (2024). FAOSTAT statistical database [Dataset]. ⟨https://www.fao.org/faostat/en/⟩.

Gaihre, Y.K., Singh, U., Islam, S.M.M., Huda, A., Islam, M.R., Sanabria, J., Satter, M.A., Islam, Md.R., Biswas, J.C., Jahiruddin, M., Jahan, Md.S., 2018. Nitrous oxide and nitric oxide emissions and nitrogen use efficiency as affected by nitrogen placement in lowland rice fields. Nutr. Cycl. Agroecosystems 110 (2), 277–291. https://doi.org/10.1007/s10705-017-9897-z.

General Statistics Office of Vietnam. (2025, May 8). Population and employment. ⟨https://www.gso.gov.vn/en/px-web/?pxid=E0201&theme=Population%20and%20Employment⟩.

Haas, E., Klatt, S., Fröhlich, A., Kraft, P., Werner, C., Kiese, R., Grote, R., Breuer, L., Butterbach-Bahl, K., 2013. LandscapeDNDC: A process model for simulation of biosphere–atmosphere–hydrosphere exchange processes at site and regional scale. Landsc. Ecol. 28 (4). https://doi.org/10.1007/s10980-012-9772-x.

Hachiya, T., Sakakibara, H., 2016. Interactions between nitrate and ammonium in their uptake, allocation, assimilation, and signaling in plants. J. Exp. Bot., erw449 https://doi.org/10.1093/jxb/erw449.

Hamada, K., Inoue, H., Mochizuki, H., Miyamoto, T., Asakura, M., Shimizu, Y., 2021. Effect of hardpan on the vertical distribution of water stress in a converted paddy field. Soil. Tillage Res. 214, 105161. https://doi.org/10.1016/j.still.2021.105161.

Houska, T., Kraus, D., Kiese, R., Breuer, L., 2017. Constraining a complex biogeochemical model for CO_2 and N_2 O emission simulations from various land uses by model–data fusion. Biogeosciences 14 (14), 3487–3508. https://doi.org/10.5194/bg-14-3487-2017.

Huong, P.T.T., Everaarts, A.P., Neeteson, J.J., Struik, P.C., 2013. Vegetable production in the Red River Delta of Vietnam. I. Opportunities and constraints. NJAS Wageningen. J. Life Sci. 67 (1). https://doi.org/10.1016/j.njas.2013.09.002.

Hutchinson, G.L., Mosier, A.R., 1981. Improved Soil Cover Method for Field Measurement of Nitrous Oxide Fluxes. Soil. Sci. Soc. Am. J. 45 (2), 311–316. https://doi.org/10.2136/sssaj1981.03615995004500020017x.

Nguyen Huy. (2025). Red River Delta transitions to a green, sustainable agriculture. Nhan Dan Online (NDO). ⟨https://en.nhandan.vn/red-river-delta-transitions-to-a-green-sustainable-agriculture-post153574.html?utm_source=chatgpt.com⟩.

Huy, D.Q., Keeni, M., Fuyuki, K., 2024. An analysis of environmental and economic impacts of the system of rice intensification: A case study in Thai Binh Province, Vietnam. Asian J. Agric. Rural. Dev. 14 (1). https://doi.org/10.55493/5005.v14i1.4983.

Intergovernmental Panel On Climate Change (Ipcc). (2019). 2019 Refinement to the 2006 IPCC Guidelines for National Greenhouse Gas Inventories: Volume 4 – Agriculture, Forestry and Other Land Use. Intergovernmental Panel on Climate Change (IPCC). ⟨https://www.ipcc-nggip.iges.or.jp/public/2019rf/pdf/4_Volume4/19R_V4_Ch11_Soils_N2O_CO2.pdf⟩.

Intergovernmental Panel On Climate Change (Ipcc), 2021. Climate Change 2021 – The Physical Science Basis: Working Group I Contribution to the Sixth Assessment Report of the Intergovernmental Panel on Climate Change, first ed. Cambridge University Press. https://doi.org/10.1017/9781009157896.

IRRI, 2024. Rice Knowledge Bank. International Rice Research Institute.

Jhang, S.-R., Chen, Y.-Y., Shiau, Y.-J., Lee, C.-W., Chen, W.-N., Chang, C.-C., Chiang, C.-F., Guo, H.-Y., Wang, P.-K., Chou, C.C.-K., 2022. Denitrifiers and Nitrous Oxide Emissions from a Subtropical Vegetable Cropland. ACS Earth Space Chem. 6 (8). https://doi.org/10.1021/acsearthspacechem.2c00106.

Johannesson, C.-F., Nordén, J., Lange, H., Silvennoinen, H., Larsen, K.S., 2024. Optimizing the closure period for improved accuracy of chamber-based greenhouse gas flux estimates. Agric. For. Meteorol. 359, 110289. https://doi.org/10.1016/j.agrformet.2024.110289.

Ju, O., Kang, N., Soh, H., Park, J.-S., Choi, E., Jeong, H., 2024. Nitrous Oxide Emissions during Cultivation and Fallow Periods from Rice Paddy Soil under Urea Fertilization. Atmosphere 15 (2). https://doi.org/10.3390/atmos15020143.

Kacjan Maršić, N., Može, K.S., Mihelič, R., Nečemer, M., Hudina, M., Jakopič, J., 2021. Nitrogen and Sulphur Fertilisation for Marketable Yields of Cabbage (Brassica oleracea L. var. Capitata), Leaf Nitrate and Glucosinolates and Nitrogen Losses Studied in a Field Experiment in Central Slovenia. Plants 10 (7). https://doi.org/10.3390/plants10071304.

Kim, G.W., Kim, P.J., Khan, M.I., Lee, S.-J., 2021. Effect of Rice Planting on Nitrous Oxide (N2O) Emission under Different Levels of Nitrogen Fertilization. Agronomy 11 (2). https://doi.org/10.3390/agronomy11020217.

Kraus, D., Weller, S., Klatt, S., Haas, E., Wassmann, R., Kiese, R., Butterbach-Bahl, K., 2015. A new LandscapeDNDC biogeochemical module to predict CH4 and N2O emissions from lowland rice and upland cropping systems. Plant. Soil. 386 (1–2). https://doi.org/10.1007/s11104-014-2255-x.

Kraus, D., Weller, S., Klatt, S., Santabárbara, I., Haas, E., Wassmann, R., Werner, C., Kiese, R., Butterbach-Bahl, K., 2016. How well can we assess impacts of agricultural land management changes on the total greenhouse gas balance (CO2, CH4 and N2O) of tropical rice-cropping systems with a biogeochemical model? Agric. Ecosyst. Environ. 224, 104–115. https://doi.org/10.1016/j.agee.2016.03.037.

Krichels, A.H., Yang, W.H., 2019. Dynamic Controls on Field-Scale Soil Nitrous Oxide Hot Spots and Hot Moments Across a Microtopographic Gradient. J. Geophys. Res. Biogeosci. 124 (11). https://doi.org/10.1029/2019JG005224.

Kritee, K., Nair, D., Zavala-Araiza, D., Proville, J., Rudek, J., Adhya, T.K., Loecke, T., Esteves, T., Balireddygari, S., Dava, O., Ram, K., S. R, A., Madasamy, M., Dokka, R. V., Anandaraj, D., Athiyaman, D., Reddy, M., Ahuja, R., Hamburg, S.P., 2018. High nitrous oxide fluxes from rice indicate the need to manage water for both long- and short-term climate impacts. Proc. Natl. Acad. Sci. 115 (39). https://doi.org/10.1073/pnas.1809276115.

Kumar, R., Mishra, J.S., Rao, K.K., Mondal, S., Hazra, K.K., Choudhary, J.S., Hans, H., Bhatt, B.P., 2020. Crop rotation and tillage management options for sustainable intensification of rice-fallow agro-ecosystem in eastern India. Sci. Rep. 10 (1). https://doi.org/10.1038/s41598-020-67973-9.

Ladha, J.K., Pathak, H., J. Krupnik, T., Six, J., Van Kessel, C., 2005. Efficiency of fertilizer nitrogen in cereal production: retrospects and prospects. In: Advances in Agronomy, 87. Elsevier, pp. 85–156. https://doi.org/10.1016/S0065-2113(05)87003-8.

Lee, Y.-J., Im, E.-C., Lee, G., Hong, S.-C., Lee, C.-G., Park, S.-J., 2024. Comparison of ammonia volatilization in paddy and field soils fertilized with urea and ammonium sulfate during rice, potato, and Chinese cabbage cultivation. Atmos. Pollut. Res. 15 (4). https://doi.org/10.1016/j.apr.2024.102049.

Lee, S., Wolberg, G., Shin, S.Y., 1997. Scattered data interpolation with multilevel B-splines. IEEE Trans. Vis. Comput. Graph. 3 (3). https://doi.org/10.1109/2945.620490.

Li, J., Wang, S., Shi, Y., Zhang, L., Wu, Z., 2021. Do Fallow Season Cover Crops Increase N2O or CH4 Emission from Paddy Soils in the Mono-Rice Cropping System? Agronomy 11 (2). https://doi.org/10.3390/agronomy11020199.

Li, X., Yuan, W., Xu, H., Cai, Z., Yagi, K., 2011. Effect of timing and duration of midseason aeration on CH4 and N2O emissions from irrigated lowland rice paddies in China. Nutr. Cycl. Agroecosyst. 91 (3). https://doi.org/10.1007/s10705-011-9462-0.

Liao, P., Sun, Y., Zhu, X., Wang, H., Wang, Y., Chen, J., Zhang, J., Zeng, Y., Zeng, Y., Huang, S., 2021. Identifying agronomic practices with higher yield and lower global warming potential in rice paddies: A global meta-analysis. Agric. Ecosyst. & Environ. 322, 107663. https://doi.org/10.1016/j.agee.2021.107663.

Linh, P. (2024, September 9). Application of technical advances to low-emission rice production in Thai Binh. *Vietnam Agriculture Newspaper (Van Nong Nghiep Moi Truong)*. ⟨https://van.nongnghiepmoitruong.vn/application-of-technical-advances-to-low-emission-rice-production-in-thai-binh-d399141.html?utm_source=chatgpt.com⟩.

Linh, T.B., Guong, V.T., Tran, V.T.T., Van Khoa, L., Olk, D., Cornelis, W.M., 2017. Effects of crop rotation on properties of a Vietnam clay soil under rice-based cropping systems in small-scale farmers' fields. Article 2. Soil. Res. 55 (2). https://doi.org/10.1071/SR16123.

Liu, X., Dai, X., Yang, F., Meng, S., Wang, H., 2023. CH4 emissions from a double-cropping rice field in subtropical China over seven years. Agric. For. Meteorol. 339, 109578. https://doi.org/10.1016/j.agrformet.2023.109578.

Luu, T.N.M., Garnier, J., Billen, G., Le, T.P.Q., Nemery, J., Orange, D., Le, L.A., 2010. N, P, Si budgets for the Red River Delta (northern Vietnam): How the delta affects river nutrient delivery to the sea. Biogeochemistry 107 (1–3), 1–3. https://doi.org/10.1007/s10533-010-9549-8.

Ma, J., Ji, Y., Zhang, G., Xu, H., Yagi, K., 2013. Timing of midseason aeration to reduce CH_4 and N_2 O emissions from double rice cultivation in China. Soil. Sci. Plant. Nutr. 59 (1). https://doi.org/10.1080/00380768.2012.730477.

Ma, R., Zou, J., Han, Z., Yu, K., Wu, S., Li, Z., Liu, S., Niu, S., Horwath, W.R., Zhu-Barker, X., 2021. Global soil-derived ammonia emissions from agricultural nitrogen fertilizer application: A refinement based on regional and crop-specific emission factors. Glob. Change Biol. 27 (4). https://doi.org/10.1111/gcb.15437.

McClain, M.E., Boyer, E.W., Dent, C.L., Gergel, S.E., Grimm, N.B., Groffman, P.M., Hart, S.C., Harvey, J.W., Johnston, C.A., Mayorga, E., McDowell, W.H., Pinay, G., 2003. Biogeochemical Hot Spots and Hot Moments at the Interface of Terrestrial and Aquatic Ecosystems. Ecosystems 6 (4). https://doi.org/10.1007/s10021-003-0161-9.

Molina-Herrera, S., Haas, E., Klatt, S., Kraus, D., Augustin, J., Magliulo, V., Tallec, T., Ceschia, E., Ammann, C., Loubet, B., Skiba, U., Jones, S., Brümmer, C., Butterbach-Bahl, K., Kiese, R., 2016. A modeling study on mitigation of N2O emissions and NO3 leaching at different agricultural sites across Europe using LandscapeDNDC. Sci. Total. Environ. 553, 128–140. https://doi.org/10.1016/j.scitotenv.2015.12.099.

Morton, L.W., 2020. Working toward sustainable agricultural intensification in the Red River Delta of Vietnam. J. Soil. Water Conserv. 75 (5). https://doi.org/10.2489/jswc.2020.0304A.

Nguyen, C., Kraus, D., Nguyen, T., Wassmann, R., Butterbach-Bahl, K., Vo, T.B.T., Mai, V. T., Bui, T.P.L., & Kiese, R. (2026, March 14). *CH4 emissions in Vietnamese Rice Agriculture: Benchmarking process-based model approaches (Tier 3) against Tier 1/2 Estimates*. https://doi.org/10.5194/egusphere-egu26-15692.

Nguyen, D.H., Scheer, C., Rowlings, D.W., Grace, P.R., 2016. Rice husk biochar and crop residue amendment in subtropical cropping soils: Effect on biomass production, nitrogen use efficiency and greenhouse gas emissions. Biol. Fertil. Soils 52 (2). https://doi.org/10.1007/s00374-015-1074-4.

Pandey, A., Mai, V.T., Vu, D.Q., Bui, T.P.L., Mai, T.L.A., Jensen, L.S., De Neergaard, A., 2014. Organic matter and water management strategies to reduce methane and nitrous oxide emissions from rice paddies in Vietnam. Agric. Ecosyst. Environ. 196, 137–146. https://doi.org/10.1016/j.agee.2014.06.010.

Pang, X., Mu, Y., Lee, X., Fang, S., Yuan, J., Huang, D., 2009. Nitric oxides and nitrous oxide fluxes from typical vegetables cropland in China: Effects of canopy, soil properties and field management. Atmos. Environ. 43 (16). https://doi.org/10.1016/j.atmosenv.2009.02.016.

Pfeifer-Meister, L., Gayton, L.G., Roy, B.A., Johnson, B.R., Bridgham, S.D., 2018. Greenhouse gas emissions limited by low nitrogen and carbon availability in natural, restored, and agricultural Oregon seasonal wetlands. PeerJ 6, e5465. https://doi.org/10.7717/peerj.5465.

Raun, W.R., Johnson, G.V., 1999. Improving Nitrogen Use Efficiency for Cereal Production. Agron. J. 91 (3). https://doi.org/10.2134/agronj1999.00021962009100030001x.

Rezaei Rashti, M., Wang, W., Moody, P., Chen, C., Ghadiri, H., 2015. Fertiliser-induced nitrous oxide emissions from vegetable production in the world and the regulating factors: A review. Atmos. Environ. 112, 225–233. https://doi.org/10.1016/j.atmosenv.2015.04.036.

Rheault, K., Christiansen, J.R., Larsen, K.S., 2024. goFlux: A user-friendly way to calculate GHG fluxesyourself, regardless of user experience. J. Open. Source Softw. 9 (96). https://doi.org/10.21105/joss.06393.

Robinson, A. (2020, June 1). Optimizing nitrogen in cabbage production. AgNet Media, Inc., (Specialty Crop Grower), Article Specialty Crop Grower. ⟨https://specialtycropgrower.com/nitrogen-cabbage-production/⟩.

Rumeau, M., Pihlblad, J., Sgouridis, F., Fereday, G., Reay, M.K., Carrillo, Y., Hartley, I.P., Sayer, E., Hamilton, L., Mackenzie, A.R., Ullah, S., 2025. Root exudate stoichiometry is a key driver of soil N cycling: Implications for forest responses to global change. Soil. Biol. Biochem., 109856 https://doi.org/10.1016/j.soilbio.2025.109856.

Sajjad, M., Hussain, K., Wajid, S.A., Saqib, Z.A., 2024. The impact of split nitrogen fertilizer applications on the productivity and nitrogen use efficiency of rice. Nitrogen 6 (1). https://doi.org/10.3390/nitrogen6010001.

Sander, B.O., Wassmann, R., Siopongco, J.D.L.C., 2016. Mitigating greenhouse gas emissions from rice production through water-saving techniques: potential, adoption and empirical evidence. In: Hoanh, In.C.T., Johnston, R., Smakhtin, V. (Eds.), Climate Change and Agricultural Water Management in Developing Countries. CABI, pp. 193–207. https://doi.org/10.1079/9781780643663.0193.

Savage, K., Phillips, R., Davidson, E., 2014. High temporal frequency measurements of greenhouse gas emissions from soils. Biogeosciences 11 (10). https://doi.org/10.5194/bg-11-2709-2014.

Schwenke, G. (2022, June 7). Nitrogen loss pathways – how much do we lose and in what form under different situations. GRDC Update Papers. ⟨https://grdc.com.au/resources-and-publications/grdc-update-papers/tab-content/grdc-update-papers/2022/06/nitrogen-loss-pathways-how-much-do-we-lose-and-in-what-form-under-different-situations⟩.

Sriphirom, P., Chidthaisong, A., Towprayoon, S., 2019. Effect of alternate wetting and drying water management on rice cultivation with low emissions and low water used during wet and dry season. J. Clean. Prod. 223, 980–988. https://doi.org/10.1016/j.jclepro.2019.03.212.

Stuchiner, E.R., Xu, J., Eddy, W.C., DeLucia, E.H., Yang, W.H., 2025. Hot or Not? An Evaluation of Methods for Identifying Hot Moments of Nitrous Oxide Emissions From Soils. J. Geophys. Res. Biogeosci. 130 (1), e2024JG008138. https://doi.org/10.1029/2024JG008138.

Sumithra, Muthayya, Sugimoto, J.D., Montgomery, S., Maberly, G.F., 2014. An overview of global rice production, supply, trade, and consumption. Ann. New. Y. Acad. Sci. 1324 (1), 7–14. https://doi.org/10.1111/nyas.12540.

Tariq, A., Larsen, K.S., Hansen, L.V., Jensen, L.S., Bruun, S., 2022. Effect of nitrification inhibitor (DMPP) on nitrous oxide emissions from agricultural fields: Automated and manual measurements. Sci. Total. Environ. 847, 157650. https://doi.org/10.1016/j.scitotenv.2022.157650.

Thanh, N. T. (2025, March 14). *Personal communication to Lara Fritzsche* [Personal communication].

Tian, H., Xu, R., Canadell, J.G., Thompson, R.L., Winiwarter, W., Suntharalingam, P., Davidson, E.A., Ciais, P., Jackson, R.B., Janssens-Maenhout, G., Prather, M.J., Regnier, P., Pan, N., Pan, S., Peters, G.P., Shi, H., Tubiello, F.N., Zaehle, S., Zhou, F., Yao, Y., 2020. A comprehensive quantification of global nitrous oxide sources and sinks. Nature 586 (7828). https://doi.org/10.1038/s41586-020-2780-0.

Tirol-Padre, A., Tran, D.H., Hoang, T.N., Hau, D.V., Ngan, T.T., An, L.V., Minh, N.D., Wassmann, R., Sander, B.O., 2017. Measuring GHG emissions from rice production in Quang Nam province (Central Vietnam): emission factors for different landscapes and water management practices. In: Nauditt, A., Ribbe, L. (Eds.), Land Use and Climate Change Interactions in Central Vietnam. Springer Singapore, pp. 103–121. https://doi.org/10.1007/978-981-10-2624-9_7.

Trang, D.M., Lan Huong, H.T., Trinh, M.V., Institute for Agricultural Environment, Vietnam Academy of Agricultural Sciences, 2019. Calculating the carbon footprint of rice production in Vietnam and formulating a proposal for mitigation options. Vietnam. J. Sci. Technol. Eng. 61 (2). https://doi.org/10.31276/VJSTE.61(2).84-89.

Trinh, M.V., Tesfai, M., Borrell, A., Nagothu, U.S., Bui, T.P.L., Quynh, V.D., Thanh, L.Q., 2017. Effect of organic, inorganic and slow-release urea fertilisers on CH4 and N2O emissions from rice paddy fields. Paddy Water Environ. 15 (2). https://doi.org/10.1007/s10333-016-0551-1.

Wang, R., Min, J., Kronzucker, H.J., Li, Y., Shi, W., 2019. N and P runoff losses in China's vegetable production systems: Loss characteristics, impact, and management practices. Sci. Total. Environ. 663, 971–979. https://doi.org/10.1016/j.scitotenv.2019.01.368.

Weier, K.L., Doran, J.W., Power, J.F., Walters, D.T., 1993. Denitrification and the Dinitrogen/Nitrous Oxide Ratio as Affected by Soil Water, Available Carbon, and Nitrate. Soil. Sci. Soc. Am. J. 57 (1). https://doi.org/10.2136/sssaj1993.03615995005700010013x.

Williams, M., 2022. Agriculture Emissions Pose Risks to Health and Climate. Rice University. ⟨https://news.rice.edu/news/2022/agriculture-emissions-pose-risks-health-and-climate⟩.

Woldendorp, J.W., 1962. The quantitative influence of the rhizosphere on denitrification. Plant. Soil. 17 (2). Article 2. JSTOR.

Xu, P., Jiang, M., Khan, I., Zhao, J., Yang, T., Tu, J., Hu, R., 2022. Available nitrogen and ammonia-oxidizing archaea in soil regulated N2O emissions regardless of rice planting under a double rice cropping-fallow system. Agric. Ecosyst. & Environ. 340, 108166. https://doi.org/10.1016/j.agee.2022.108166.

Yi, Z., Jeyakumar, P., Yin, C., Sun, H., 2023. Effects of biochar in combination with varied N inputs on grain yield, N uptake, NH3 volatilization, and N2O emission in paddy soil. Front. Microbiol. 14, 1174805. https://doi.org/10.3389/fmicb.2023.1174805.

Zhang, L., Yuan, J., Zhang, M., Zhang, Y., Wang, L., Li, J., 2022. Long term effects of crop rotation and fertilization on crop yield stability in southeast China. Sci. Rep. 12 (1). https://doi.org/10.1038/s41598-022-17675-1.

Zhao, C., Qiu, R., Zhang, T., Luo, Y., Agathokleous, E., 2024. Effects of alternate wetting and drying irrigation on methane and nitrous oxide emissions from rice fields: a meta-analysis. Glob. Change Biol. 30 (12). https://doi.org/10.1111/gcb.17581.

Zou, J., Huang, Y., Zheng, X., Wang, Y., 2007. Quantifying direct N2O emissions in paddy fields during rice growing season in mainland China: Dependence on water regime. Atmos. Environ. 41 (37). https://doi.org/10.1016/j.atmosenv.2007.06.049.